COBALT ADSORPTION AND/OR CO-PRECIPITATION ONTO FERRIC OXYHYDROXIDE

by

Lun Wei Su

B.Sc., Simon Fraser University,

Vancouver, 2008

A THESIS SUBMITTED IN PARTIAL FULFILLMENT OF THE REQUIREMENTS FOR THE DEGREE OF

MASTER OF SCIENCE

in

The Faculty of Graduate Studies

(Materials Engineering)

THE UNIVERSITY OF BRITISH COLUMBIA

(Vancouver)

July 2011

ABSTRACT

The Caron process was developed in the 1920s. In this process, the ore is dried and milled, then roasted in a reducing atmosphere to convert nickel and cobalt to their metallic form. Nickel and cobalt are then leached in ammoniacal solution but some losses occur due to adsorption and co-precipitation with iron oxide or hydroxide precipitates. The effects of various parameters on iron precipitation in the Caron process leach were studied. The parameters studied include pH, temperature, contact time with iron and its precipitates and initial ferrous concentration. The adsorption of otherwise soluble Co onto freshly precipitated ferric hydroxide was measured at four different temperatures between 20ºC and 35ºC. The percentage of cobalt adsorbed onto iron precipitates was directly related to the initial iron concentration but the effect of temperature was less clear. The amount of cobalt adsorbed depended on the pH. Solution contact time with iron precipitates had a very small effect on cobalt adsorption (2-3% difference). The highest adsorption of cobalt (99%) was obtained with an initial concentration of 0.2 M ferrous sulfate at pH 7 after 2 hours of contact time. The main iron precipitate was ferrihydrite. X-ray analysis revealed the characteristic “2 line” ferrihydrite ($Fe_5HO_8 \cdot 4H_2O$) with no goethite being observed in any of the precipitates. TEM revealed an amorphous structure, which is also indicative of ferrihydrite. SEM showed a preponderance of poorly resolved precipitates, which did not appear to be crystalline. Traces of cobalt were measured in the ferrihydrite particulate by EDX.

TABLE OF CONTENTS

LIST OF TABLES

LIST OF FIGURES

LIST OF EQUATIONS

ACKNOWLEDGEMENTS

First of all, I wish to extend my heartfelt gratitude to my supervisor Dr. Edouard Asselin for his helpful support and guidance throughout the last two years so that I can successfully complete this work. Also, I would like to express my thankful gratitude toward Dr. Berend Wassink for lending me the technical instruments and Dr. Akram Alfantazi for the thoughtful discussion and ideas.

I also extend my sincere thanks to Mary Fletcher for helping me using the instruments such as SEM. Special thanks to my colleagues, Ahmad Ghahremaninezhad, Fernado Parada and Subrata Roy for their assistances and support.

I sincerely thank all the people who have given me technical support and thoughtful ideas. Finally I would like to thank my parents and my wife for their consistence love and support.

DEDICATION

To parents, my wife, and my lovely daughter Evelyn

"*I love you all"*

1. INTRODUCTION

Laterite ores of Ni have recently received a lot of attention due to the growing demand for stainless steel and the decline of sulphide ore deposits. [Pickles, 2004 and Lee et al., 2005] It has been reported that laterites contain about 70% of the world's land based nickel resources. However, only 40% of the world nickel production is currently from lateritic sources. [Dalvi et al., 2004] At the top layer of laterite ore bodies, oxidic type ores such as limonites and silicates are found. [Liu and Hernandez, 2009] Since the quantity ratio of iron to nickel concentration is high in laterites and since iron dissolves readily in acidic hydrometallurgical solutions, the deportment of iron has a significant effect on process control and selection.

At present, several methods have been developed for the recovery of nickel and cobalt from lateritic ores. A variety of flow sheets are used to process laterite ores: (a) pyrometallurgical processes (b) hydrometallurgical processes and (c) a mixed pyro-hydrometallurgical process – the Caron process [Liu and Hernandez, 2009]. Pyrometallurgical processes include the production of ferronickel and matte smelting, which involves drying, calcining/reduction and electric furnace smelting. Hydrometallurgical processes are more applicable to the limonite fraction of laterite deposits, which is the high iron laterite, and include atmospheric leaching with sulphuric acid (AL) and high pressure acid leaching (HPAL). [Guo at el., 2009] The limonite zone, characteristic of humid, well-drained regions, is dominated by goethite, FeOOH. Pyrometallurgical processes such as smelting are suited for ores containing predominately

saprolite, which contain lower amounts of cobalt and iron. These processes are energy intensive since all the free moisture must be removed through calcination and the calcine must be melted to form a slag at around 1600°C. HPAL, the most common hydrometallurgical approach, involves leaching of slurried ore with sulphuric acid at elevated temperatures and pressures which causes almost total dissolution of the feed material followed by precipitation of iron as hematite. The Caron process can be used for limonitic ores or a mixture of limonite and saprolite. In this process, the ore is dried at 700°C and nickel is selectively reduced together with cobalt and some iron to form a metallic alloy. The metallic components are then extracted by leaching in an ammoniacal solution. The disadvantages of the Caron process are related to the front-end steps such as ore drying and reduction, which are energy intensive. [Liu et al., 2009; Reid and Barnett, 2002] While, HPAL yields much higher nickel and cobalt dissolution with only half to one third of the required energy of the Caron process, it also requires expensive autoclaves and high maintenance costs. [Liu et al., 2009; Guo et al., 2009; Reid and Barnett, 2002]

The low recoveries of cobalt in the Caron process are believed to be due to the passivation of the Fe-Ni-Co alloy, which is formed during the reduction step and/or its co-precipitation or adsorption on iron hydroxide. [James and Healy, 1972] During the leach, the iron that is reduced undergoes dissolution as a ferrous ammine species, which can oxidize to the ferric state and precipitate out as hydrated oxides. [Crawford et al., 1997] Mr. Subrata Roy (2010) has already discussed the passivation of iron in Caron solutions and its

possible effect on cobalt dissolution. The current thesis investigates the adsorption and co-precipitation at Co onto Fe oxides and/ or hydroxides. Hence a review of the Caron process and the concepts of cobalt adsorption and co-precipitation on iron oxide are studied in Chapter 2. In Chapter 3, a brief research objective will be introduced, while in Chapter 4 and Chapter 5, the experiment procedure and experimental results will be discussed respectively. Finally in Chapter 6, a conclusion based on experimental results will be made.

2. LITERATURE REVIEW

2.1 Laterite Ore

Laterite nickel and cobalt ore generally contain limonites, which is an oxidic type of ore. Limonites usually can be found at the top layer of ore body whereas silicate type of ores is found at the bottom layer of ore body. A transition zone separates these two states. Limonite and saprolite contains either ferric ions of iron and /or ferrous iron depending on the geological history of weathering and oxidation. Magnetite Fe_3O_4 was found in the less weathered or oxidized limonite. The less weathered or oxidized saprolite has greenish color and it is defined as the lower saprolite. [Liu and Hernandez, 2009] Laterites can be found in different places around the world. The chemical compositions of each laterite ores are shown in Table 2.1. [Liu and Hernandez, 2009]

Table 2.1: Chemical composition of laterite ore [Liu and Hernandez, 2009]

Laterite Ore	**Total Fe**	**Fe^{2+}**	**Mg**	**Ni**	**Co**
Indonesian limonite	40.8	nd	1.3	1.53	0.10
Indonesian saprolite	8.5	nd	14.6	3.37	0.03
New Caledonia limonite	47.1	nd	0.4	1.33	0.16
New Caledonia saprolite	7.7	nd	23.3	1.00	0.02

Laterite Ore	**Total Fe**	**Fe^{2+}**	**Mg**	**Ni**	**Co**
Western Australia low-Mg ore	25.4	nd	4.9	2.50	0.07
Western Australia high-Mg ore	10.0	nd	16.6	1.38	0.02
Southern American partially oxidized saprolite	30.60	8.36	3.98	1.38	0.10
Southern American partially oxidized limonite	14.38	4.93	15.53	0.96	0.04
Southern American partially oxidized laterite composite of limonite and saprolite	22.6	6.6	6.9	1.30	1.10

Saprolites with high nickel content are usually used in pyrometallurgical process such as the RKEF process, which involves roasting ore inside of rotary kin. It also required electrical furnace smelting techniques to produce ferronickel. This process involves a drying step, a reduction roast step to convert the nickel oxide to nickel, and smelting in an electrical furnace. A high-grade saprolite source is required to make it economically feasible and has a disadvantage that financial value of any cobalt in the ore is recovered into the ferro-nickel. [Liu and Hernandez, 2009]

Limonites consist of a mixture of hydrated iron (III) oxihydroxides of varying composition to which a generic formula can be assigned: $FeO(OH) \cdot nH_2O$. Limonite deposits can be found in iron bearing limestone. The iron content is gradually dissolved by circulating waters and transported to favorable spots. Then iron slowly re-deposits as limonite and replaces the calcium carbonate of the rock. Limonite is heavy and yellowish-brown and it mixes with fine clay to make what is known as yellow ocher. [Liu and Hernandez, 2009]

2.2 Caron Leaching and the Caron Process

The Caron process has been practiced in Australia (Greenvale-Yabulu), Brazil (Niquelandia) and Cuba (Nicaro) [Nicol et al., 2010]. The reduction of nickel laterite ores usually happens at around 750°C. The Caron process can be briefly defined as the oxidative dissolution of pre-reduced iron based nickel-cobalt-copper alloys in ammoniacal carbonate solution at atmospheric temperature. [Caron, 1950] A flowsheet of the Caron process is shown in Figure 2.1. The abbreviated form of the Caron process is indicated in operations (1) to (4). Laterite nickel ore (1) is reduced and then leached by an ammoniacal ammonium carbonate leach solution (2) to produce ore tailings (B) and process liquor (4). The feed ammoniacal ammonium carbonate leach solution of the process is the process liquor (4). The process liquor originating from the leach contains 8-16% ammonia, 4-12% carbon dioxide, 0.5-1.5% nickel and 0.02-

0.2% cobalt. A portion of the ammoniacal ammonium carbonate leach solution containing some nickel and cobalt is treated with ammonium hydrosulphide (A) to produce a solid precipitate of mixed cobalt/nickel sulphide (5). Mixed cobalt/nickel sulphide reductant slurry (5a) is transferred and then added together with mixed nickel/cobalt hydroxide feed (7) and the feed ammoniacal ammonium carbonate leach solution. The nickel and cobalt from both the mixed hydroxide and the added mixed sulphide reductant are leached into the product solution with some minor impurities in the form of manganese, magnesium and iron from the mixed hydroxide. The enriched product liquor (9) is separated from the residue (8) and then added to the remaining process liquor. The further processing (9) is used to separate and extract the nickel and cobalt. The leach residue (8) is rejected and/or recycled to the ore treatment section. [Anderson et al., 1960]

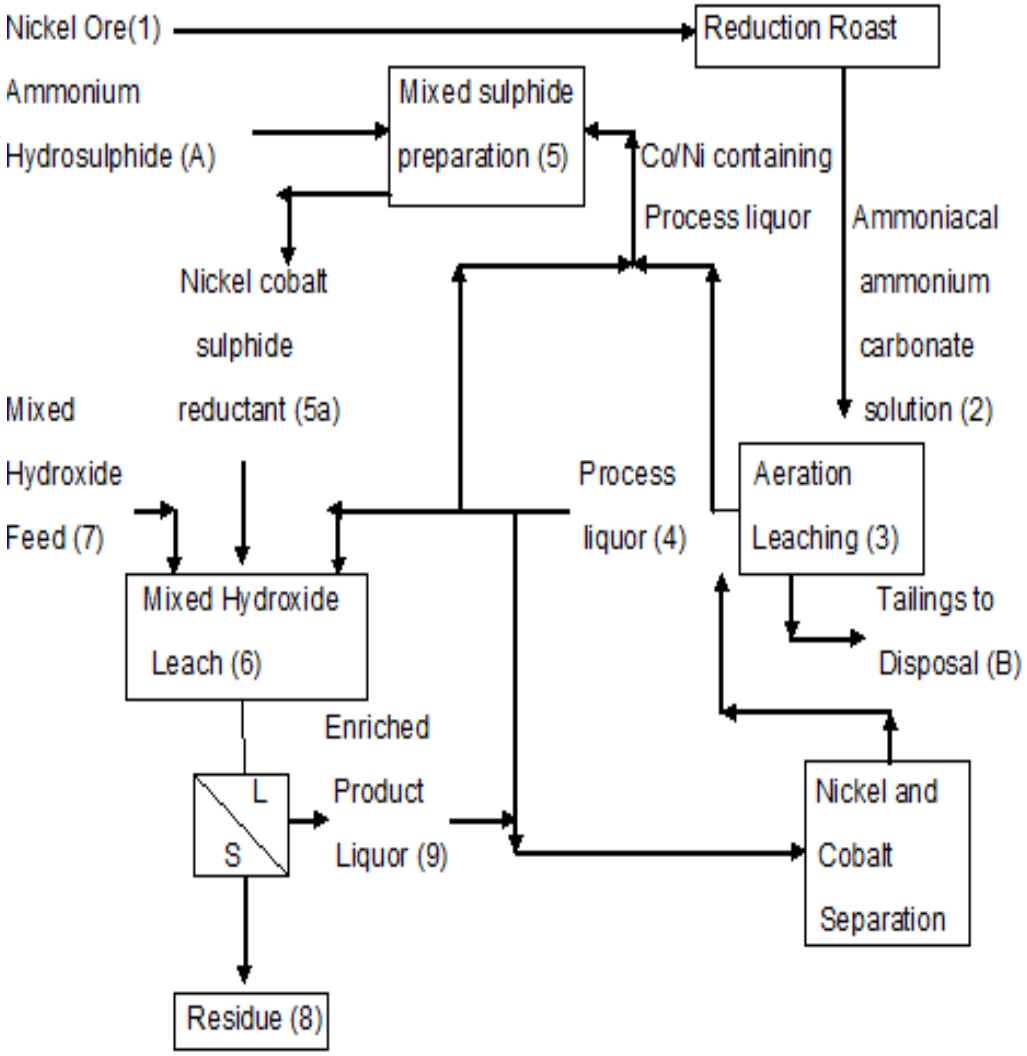

Figure 2.1: Flowsheet of the Caron process with single stage leach [Osseo-Asare, 1981]

2.3 Advantages and Issues of Concern in the Caron Process

a) The energy consumption is high in the drying and roasting processes, compared to the direct atmospheric or high pressure leaching of nickel laterites; [Xavier and Ciminelli, 2008]

b) Much of the iron is converted to Fe_3O_4 in the roaster, whereas Fe_2O_3 is precipitated in high-pressure acid leaching processes. Some unreduced Ni-Co-oxides can be entrapped in Fe_3O_4, which can lead to low efficiency nickel and cobalt leaching. [Nicol et al., 2010]

c) The two main reagents are NH_3 and CO_2 and they can be recovered for leaching with insignificant energy costs associated with recycling; [Muri and Ho, 2006]

d) The tailings contain high levels of nickel and cobalt; [Nicol et al., 2010]

e) The leach has slow kinetics and only 80-86 % Ni and 50-60% Co are recovered; [Nikoloski, 2002; Nicol et al., 2004]

f) There is a high selectivity of nickel and cobalt over iron; [Burkin, 1987]

There are different reasons put forward to explain the low metal recovery in the Caron process:

1) Less reactive nickel sulfide is formed during reduction roasting with sulfur-containing fuel oil; [Prado and Dempsey, 1986]

2) Passivation or surface blockage of ferronickel by iron oxides or sulfides; [Kim et al., 1991; Nikoloski, 2002; Nicol et al., 2004] Ferronickel may form an inert oxide and any "$Fe(OH)_3$" precipitate may coat the unreduced ore particles and interfere with nickel or

cobalt leaching in the Caron process; [Kim et al., 1991] To avoid passivation of the hot ferronickel intermediate, the roaster product is first leached in an anaerobic atmosphere. An aerobic integrated leaching train follows this. Typical leaching conditions include leach liquors at less than 45°C containing 5.29 M NH_3, 1.02 M HCO_3^-, 15.33 mM Ni (II), 11.88 mM Co (III), 22.32 mM $S_2O_3^{2-}$ and 0.79 to 15.74 mM Cu, as well as SO_4^{2-} and other metal ions such as Fe (II) and Mn (II) [Nikoloski, 2002, Nicol et al., 2004]

3) The adsorption of metal ammine complexes by oxides and/or hydroxides; [Caron, 1950; Osseo-Asare and Fuersteneau, 1987, 1979, 1980; De Graff 1979; Han et al., 1982; Mehta and Han, 1984]

2.4 Role of Iron

A Ni-Co-Fe alloy is formed during the reductive roast. This alloy dissolves in the leaching process and Ni and Co ammines complexes are stabilized in solution. The iron is then precipitated as an oxyhydroxide, hopefully leaving the Ni and Co in solution. [Osseo-Asare and Fuerstenau, 1979] Alloys of iron with nickel, cobalt or copper undergo passivation at potentials typical of the Caron process, which inhibits further dissolution of these metals trapped within the passive iron alloy matrix. [Crawford et al., 1997]

Nicol et al. have suggested that sulphide species may play a role in Caron leach passivation. Indeed, the initial product of ammoniacal leaching of nickel sulphides is known to be thiosulfate. Thiosulfate is subsequently oxidized to polythionates, then to sulphamate and sulphate. [Muir et al., 1981] Since oxygen will swiftly oxidize Co (II) to Co (III) and the concentration of Co (III) as the oxidizing agent will be higher than the concentration of dissolved oxygen, the ammine complex of Co (III) will act as a redox mediator for nickel. Thiosulfate is found to be the major sulfoxy species due to the utilization of sulphur-containing oil in the roaster, which may result in the formation of nickel sulphides during roasting. The formation of nickel sulphide causes the passivation of ferronickel active sites. [Davis and Leckie. 1978]

The passivation of iron was investigated electrochemically by Nikoloski and his co-workers (2003) during the leaching of pre-reduced laterite ores in ammoniacal solutions. With the presence of thiosulphate, the highest current densities were obtained which indicated that the presence of thiosulphate facilitated the dissolution of the iron. Thiosulfate is found to be the major sulfoxy species in the Caron leach liquor due to the utilization of sulfur-containing oil [Reid and Fittock, 2004] Thiosulfate may form nickel sulfate during roasting. [Prado and Dempsey, 1986] This nickel thiosulfate may cause the passivation of ferronickel active sties in which thiosulfate is responsible for the low recovery of nickel. [Nikoloski, 2002] It has been reported that passivation similar to that for iron metal are also exhibited by both nickel and cobalt albeit at higher potentials.

In addition to the possibility of iron passivation, co-precipitation or adsorption with/onto iron oxyhydroxides has also been blamed for low cobalt and nickel recoveries.

2.5 Theory of Adsorption and/or Co-precipitation

Precipitation, adsorption, and co-precipitation of heavy metals are increasingly important in many technological processes such as the formation of ceramic and metallic precursors. They are also used to remove heavy metals from wastewater streams. [Crawford, 1993] There is not a clear distinction between precipitation, co-precipitation and adsorption and these basic processes are defined in Figure 2.2

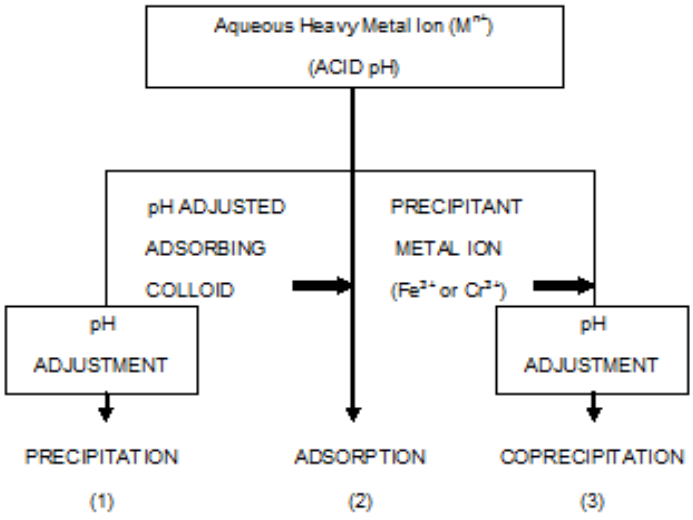

Figure 2.2: Schematic representations of the three processes responsible for the removal of heavy metal ions from solution.

With an increasing of pH, the heavy metal ions will eventually result in the formation of an insoluble metal hydroxide precipitate. At very high pH, re-dissolution of the metal hydroxide may occur. When a solid substrate surface is present, adsorption may also occur. In the case of adsorption, the solid substrate is preformed prior to addition of the metal ion to be removed from solution. Whereas co-precipitation processes are subtly different to adsorption processes.

In the case of co-precipitation, the solid substrate is formed in the presence of the metal ion to be removed from solution. [Crawford et al., 1993] However, the relationship between co-precipitation and adsorption is not clear, but co-precipitation often removes metals to an even greater extent than direct adsorption. This enhancement can be due to either greater binding strength for a co-precipitation surface since it has multiple surface site types over a simple precipitate surface, which has a single surface type [Crawford et al., 1993]

For example, the precipitation, adsorption, and co-precipitation using amorphous iron (III) oxide as the adsorbing or co-precipitated colloid are shown in Figure 2.3 for Ni (II). The precipitates may contain ferrihydrite and iron oxide. In this case, the concentration of Ni (II) in the aqueous phase changed from the initial added Ni (II) concentration to zero over a narrow pH range of 6.8-8.2, which agrees with the findings of Osseo-Asare and Fuerstenau (1979) for Ni (II) adsorption onto hematite. In any case, co-precipitation is more efficient for metal removal than adsorption and precipitation. [Crawford et al., 1993]

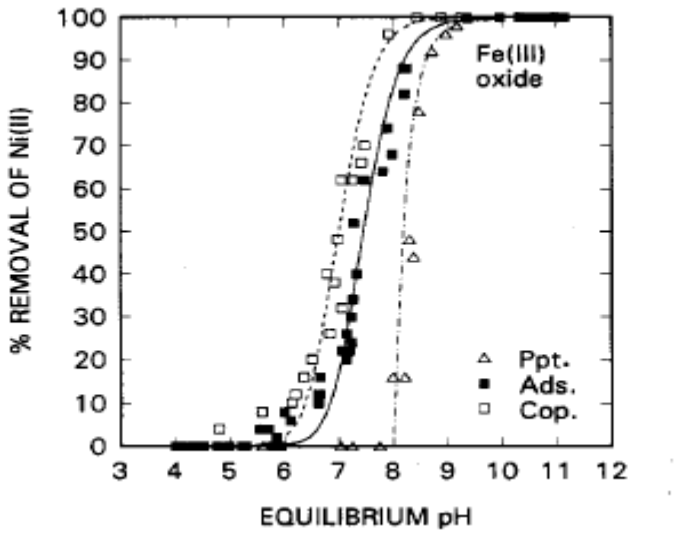

Figure 2.3: Adsorption and co-precipitation of Ni (50ppm) with amorphous iron (III) oxide (250ppm) compared to precipitation of Ni (50ppm) alone. [Crawford et al., 1993]

2.6 Adsorption and/or Co-precipitation of Heavy Metal on Fe Oxides/Hydroxides

The removal of iron in hydrometallurgical processing is a critical step and is usually achieved through precipitation of iron oxyhydroxides. A high supersaturation environment for precipitation can readily be created due to the very low ferric-ion solubility (<0.06 mgL^{-1} at pH 4-10) and results in nucleation of nanoscale phases such as 2-line ferrihydrite with rapid hydrolysis (often referred to as HFO), 6-line ferrihydrite if hydrolysis proceeds slower, [Schwertmann et al., 1999] Schwertmannite ($Fe_{16}O_{16}(SO_4)_2(OH)_{12}$), and poorly crystalline goethite. [M. Loan et al., 2002] The rapid aggregation of primary

ferrihydrite crystals to form aggregates (up to 100µm in size) creates both internal and inter-particle micro-porosity and surface areas can exceed 200 m^2g^{-1}. Ferrihydrite, in particular, is known to absorb a wide range of inorganic and organic species [Cornell and Schwertmann, 2003; Dutrizac and Jambor, 1998] Ferrihydrite is generally the first product of ferric hydrolysis in acid media. In fact the ferric hydroxide ($Fe(OH)_3$) that has been described in the hydrometallurgical literature is almost certainly ferrihydrite. [Dutrizac and Jambor, 1998; Dutrizac and Zinck, 1998] It is often referred to as amorphous, however, ferrihydrite is not strictly amorphous since it has a very small primary particle size (1-7 nm) and the broad reflections in an XRD pattern are the result of short-range structural order.

Thus ferrihydrite ($Fe_5HO_8.4H_2O$) is a disordered and metastable Fe(III) oxyhydroxide mineral. The nomenclature 'ferrihydrite' refers to a range of similar phases. 2-line and 6-line are the common forms of ferrihydrite. The prefix here represents the number of broad reflections observed in diffraction patterns. [Dutrizac and Jambor, 1998] Ferrihydrite undergoes transformation to more crystalline products of goethite (α-FeOOH) and hematite (α-Fe_2O_3) and this can be significantly affected by changes in pH, temperature and water activity. [M. Loan et al., 2006]

The characteristic XRD patterns for ferrihydrite are shown in Figure 2.4. As mentioned above, ferrihydrite comes in two forms: "2-line ferrihydrite" and "6-line ferrihydrite". The majority of the studies in the area of Co and Ni loss by precipitation in the Caron leach have focused on iron oxide phases such as

hematite but it is also possible that ferrihydrite could form under Caron conditions.

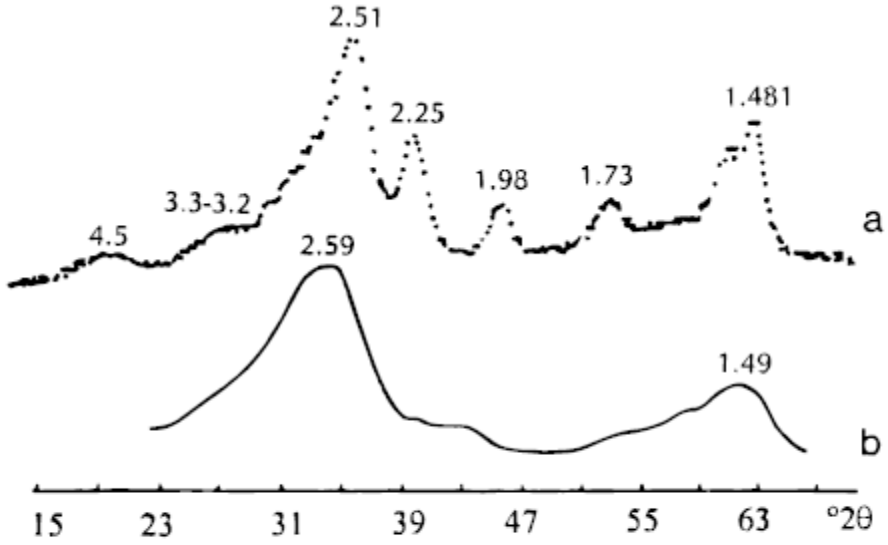

Figure 2.4: Experimental XRD patterns for 6 (a) and 2-line (b) ferrihydrite. Cu Kα radiation. [Dutrizac and Jambor, 1998]

The low recoveries of cobalt and nickel in ammoniacal solution have historically been attributed to their interaction with iron oxyhydroxides and manganese oxide leach residues. Different kinds of oxidic products can form in the Caron leach through a series of reactions similar to those presented below: [Osseo-Asare, 1980]

$$Fe + 4NH_3 + ½\ O_2 + 2H^+ = Fe(NH_3)_4^{2+} + H_2O \qquad 2\text{-}1$$

$$Fe(NH_3)_4^{2+} + 2H_2O = Fe(OH)_2(s) + 4NH_3 + 2H^+ \qquad 2\text{-}2$$

$$Fe(NH_3)_4^{2+} + 1/4\ O_2 + 1/2\ H_2O + 2OH^- = Fe(OH)_3(s) + 4HN_3 \qquad 2\text{-}3$$

$$3Fe(NH_3)_4^{2+} + 1/2\ O_2 + 6OH^- = Fe_3O_4 + 12NH_3 + 3H_2O \qquad 2\text{-}4$$

$$2Fe(NH_3)_4^{2+} + 1/2\ O_2 + 4OH^- = Fe_2O_3 + 8NH_3 + 2H_2O \qquad 2\text{-}5$$

Ferrihydrite precipitation is not mentioned in the reactions above, as it has been common to erroneously associate ferric precipitation with a generic ferric hydroxide (reaction 2-3). As the reader will see, it appears as though ferrihydrite may be a major precipitation product in the Caron leach. Caron (1950) has suggested that cobalt is lost from leach liquor by adsorption and coprecipitation processes associated with the iron oxide precipitates formed during the leaching operation. Osseo-Asare and Fuerstenau (1979) have pointed out that the adsorption behavior of cobalt, nickel and copper on hematite, rutile, alumina and quartz was affected by the pH of the solutions.

Adsorption of trace heavy metals onto solid phases is important in controlling heavy metal activity and it is governed by the composition of solid phases, particularly the content of metal oxides such as iron oxides. [Nelson et al., 2001] Duval and Kurbatov reported that the amount of ferric oxide had significant effect on cobalt and barium adsorption. Cobalt had higher adsorption than barium under comparable conditions. This was because cobalt had smaller atomic size than barium. In addition, when pH was below 7, the adsorption was strongly dependent on other factors such as chloride ion concentration. The hydrolysis of cobalt ion was the main factor for its adsorption by hydrous ferric oxide. [Duval and Kurbatov, 1952]

There is also research that focuses on the influence of temperature on the adsorption of cadmium (II) and cobalt (II) on goethite. The adsorption of Cd

(II) and Co (II) onto goethite at five temperatures between 10 and 70ºC was investigated. In this research, Langmuir and surface complexation methods were used. The adsorption was shifted to lower pH as the temperature was increased. When the pH reached 8.5, both Co and Cd were fully adsorbed at all temperatures. The result of adsorption isotherms had shown that the adsorption of Cd (II) and Co (II) onto goethite was temperature dependent and more Co (II) was adsorbed to the goethite surface at low cation concentrations. [Angove et al., 1999] The analysis of Cd (II) and Co (II) adsorption at pH 7 showed more Co was adsorbed than Cd (II). [Angove et al., 1999]

Landry and his co-workers (2009) measured the Co adsorption as a function of pH, ionic strength and sorbate to sorbent ratio on hydrous ferric oxides (HFO), kaolinite and quartz. The surface complexation model was used. Double layer model (DLM) was chosen for surface complexation model, which was due to its availability of datasets for metal adsorption on HFO and hydrous manganese oxide. DLM is one of the thermodynamically based surface complexation models (SCMs). Co adsorption was measured on HFO as a function of pH, ionic strength and sorbate/sorbent ratio on pure quartz, HFO and kaoline and on binary and ternary mixtures of the three solids. In order to obtain an accurate prediction of Co sorption over wide ranges of ionic strength and sorbate/sorbent ratio, it may require ionic-strength dependent stability constants for DLM. In this experiment, DLM stability constants for Co sorption derived for pure solids were used to predict sorption as a function of pH and solid concentration on binary and ternary mixtures of the three solids. The

experiment results showed that as the ionic strength increased to 0.1M, the pH at which 50% of Co was adsorbed increased from 6.06 to 6.33. Decreasing the sorbate/sorbent ratio by two orders of magnitude from 10^{-4}M Co to 10^{-6}M Co with 2gL^{-1} HFO and increasing the solid concentration from 2 to 5 gL^{-1} with 10^{-5} M Co and 0.1 or 0.01M $NaNO_3$ had little effect on the adsorption edge. Adsorption of Co on hydrous ferric oxide (HFO) was the subject of study by Dzombak and Morel. (1990) They assumed that Co adsorption on HFO could be described using a 2-site model with formation of monodentate Co surface complexes according to the following equations:

$$Fe_{(s)}OH + Co^{+2}_{(aq)} \rightarrow Fe_{(s)}OCo^{+} + H^{+}(aq) \qquad 2\text{-}6$$

$$Fe_{(w)}OH + Co^{+2}_{(aq)} \rightarrow Fe_{(s)}OCo^{+} + H^{+}(aq) \qquad 2\text{-}7$$

90-95% of the Co adsorbed in these experiments within 5 hours and 100% adsorption occurred after 30 hours.

Mehta and Han (1984) have studied the selective adsorption of copper, nickel, cobalt and other transition metal ions from sulfuric acid solutions with the chelating ion exchange resin XFS 4159. The distribution behavior of the cations of copper (II), nickel (II), cobalt (II) and iron (II) was studied. XFS 4195 has been known to absorb transition metal cations such as nickel, cobalt and copper. The effects of pH and metal ion concentration were studies. However, at higher pH values, there was no pH dependence. [Grinstead, 1984] The metal ions were adsorbed in the order of Ni, Fe(III), Zn, Co, Cd and Fe(II). For the distribution of copper, there was a very strong affinity of XFS 4195 in the pH 2

isotherm. Aluminum and Iron (III) had less effect on copper loading and copper was not readily eluted with acid eluants but it was eluted with dilute ammonium hydroxide. The distribution of nickel was not affected by the presence of sulfate derived from aluminum or magnesium. However, the use of ammonium sulfate reduced nickel adsorption. The cobalt adsorption was reduced in the presence of iron (III) and the resin absorbed iron. The literature is clear on the fact that at the pH value for which multivalent cations hydrolyze, there is a remarkable increase in adsorption. [Mehta and Han, 1984; Grinstead, 1984]

Also, in another Mehta and Han (1984) study of selective removal of Co(II) from Ni(II) by coprecipitation with manganese in ammoniacal solutions, they pointed out that as the pH of solution is higher, there are more amounts of coprecipitation of cobalt and nickel which is shown in Figure 2.5. It was also found that as the total ammonia concentration increased from 0.5 to 2.0M, the amount of coprecipitation decreased and this change is pronounced at pH 9.5.

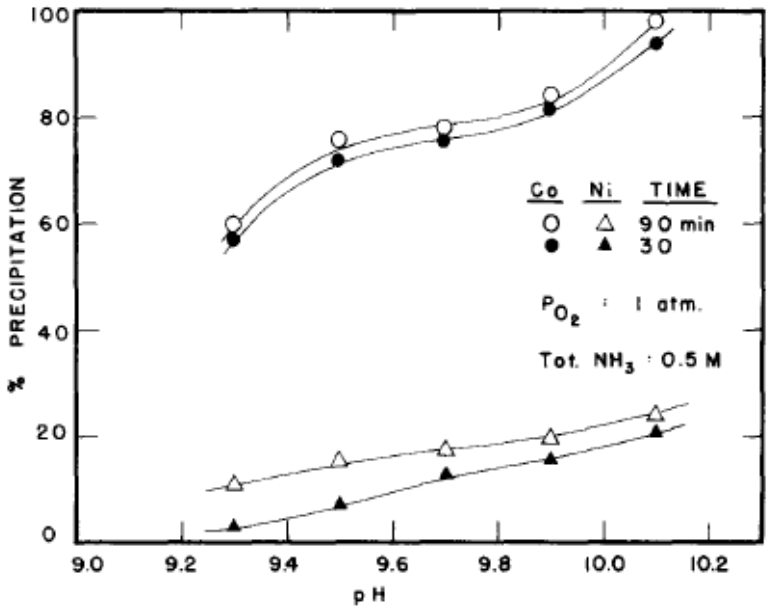

Figure 2.5: Effect of pH on coprecipitation of Co(II) and Ni(II) with manganese [Mehta and Han, 1984]

At the pH value for which multivalent cations hydrolyze, there is a remarkable increase in adsorption. Multivalent cation adsorption is often carried out at pH below the pH_{pzc}. The pH dependence of metal adsorption is influenced by two factors. One factor is solubility and distribution of metal ions in the solution and the other factor is the overall charge of the adsorbent. From the perspective of surface charge of adsorbent, the pH of maximum metal uptake is very close to pH_{pzc} of cobalt. Osseo-Asare and Fuerstenau studied the uptake of copper, nickel, and cobalt by various adsorbents as a function of pH and ammonia concentration in aqueous ammonia systems relevant to the Caron process. The adsorption of Cu and Co was very rapid but Ni uptake was slower. The concentration of hematite was varied in order to determine how the total surface area of the dispersed solids affects the adsorption process. As a

result, metal loss from solution increased as the solid-to-liquid ratio increased. [Osseo-Asare and Fuerstenau, 1979] The effect of pH and ammonia concentration on the adsorption of cobalt by the hematite adsorbent is shown in Figure 2.6 and Figure 2.7.

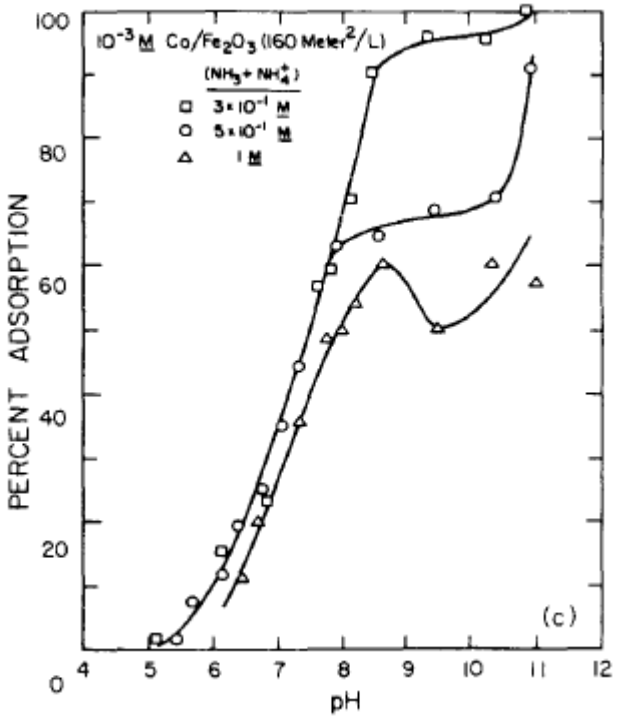

Figure 2.6: The uptake of cobalt from $10^{-3}M$ metal solutions by hematite (160 m^2/liter) as a function of pH at various concentrations of total ammonia [Osseo-Asare and Fuerstenau, 1987]

Ossseo-Asare and Fuerstenau (1987) found that as the total ammonia concentration was increased, metal uptake decreased and as the pH increased up to pH 7, the amount of dissolved cobalt taken up by the solids increased at 0.5 M of total ammonia concentration.

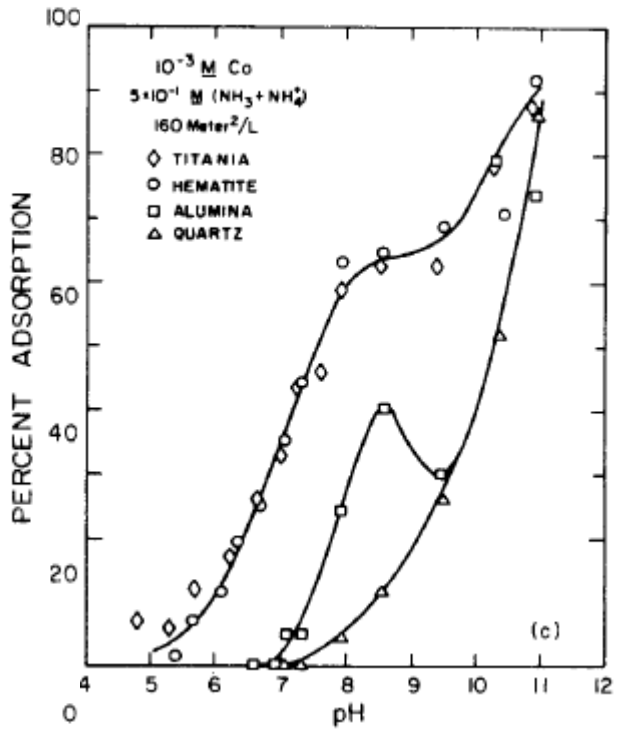

Figure 2.7: The uptake of cobalt from 10^{-3} *M* metal solutions by various substrates (160 m^2/liter) as a function of pH at 0.5 *M* total ammonia [Ossseo-Asare and Fuerstenau, 1987]

Landry et al. (2009) have also confirmed that the amount of Co(II) and Ni(II) co-precipitation decreased as the total ammonia concentration increased at constant pH.

Furthermore, it is known that elements such as nickel and cobalt are often associated with manganese as well as iron. Hence cobalt can co-precipitate not only with iron but also with manganese. There is a research which focuses on the selective removal of Co(II) from Ni(II) by coprecipitation with manganese in ammoniacal solution, the effect of oxygen on coprecipitation and the conditions for efficient recovery were investigated. The rate of

precipitation of manganese was independent of pH between pH of 9.3-10.1. [Mehta and Han, 1984]

According to the above review of adsorption processes, the relevant studies have some commonalities. Metal uptake will generally increase as pH increases. Cobalt adsorption increases steadily with time. Increased ammonia concentration decreases the tendency for adsorption/co-precipitation. Temperature has a marginal effect on cobalt adsorption.

3. RESEARCH OBJECTIVES

The recoveries of cobalt in the Caron process are low. This is due to the passivation of the Fe-Ni-Co alloy formed during the reduction step and the co-precipitation or re-adsorption of cobalt into/onto iron oxyhydroxides. [James and Healy, 1972] The objective of this work is to perform cobalt precipitation studies in ammoniacal solutions containing with higher total amounts of ammonia than in previous studies to identify the extent of cobalt loss in simulated Caron solutions.

4. EXPERIMENTAL PROCEDURE

4.1 Co-precipitation

The ammoniacal ammonium carbonate solutions were prepared using a total ammonia concentration, NH_3, of 6.5 M and Co concentration of 0.01 M. The solution was stirred for one hour. Argon gas was sparged into the cobalt solution (200 mL) to remove O_2 for half an hour. Iron (II) sulfate ($FeSO_4 \cdot 6(H_2O)$) was then added to the cobalt bearing solution and air was sparged into the solution for two hours as shown in Table 4.1. All co-precipitation experiments were done using the same procedure but with different contacting times where the oxygen supply (air) was added for different time periods. The temperature of the solutions was controlled by a water bath supplying water through a jacketed cell and the temperatures for the experiments were 20, 25, 30, and 35ºC. A sample of the cobalt solution was gathered through a syringe filter (0.2 µm) after two hours. The precipitate was dried in the oven for 24 hours at 40°C and then weighed.

Table 4.1: Experimental conditions

Contacting Time (Hours)	**Temperature (°C)**	**Fe(II) Concentration (M)**	**Cobalt Concentration (M)**	**pH**
1	25, 30, 35	0.05, 0.1, 0.15, 0.2	0.01	10

Contacting Time (Hours)	Temperature (°C)	Fe(II) Concentration (M)	Cobalt Concentration (M)	pH
2	25, 30, 35	0.05, 0.1, 0.15, 0.2	0.01	10
4	25, 30, 35	0.05, 0.1, 0.15, 0.2	0.01	10

To determine the effect of pH, the cobalt-containing ammoniacal ammonium carbonate solutions were prepared as above except that sulfuric acid (6M) was used to adjust the pH. The test solution pH was adjusted to 6, 7, 8, 9, and 10. Three experiments are done for each condition.

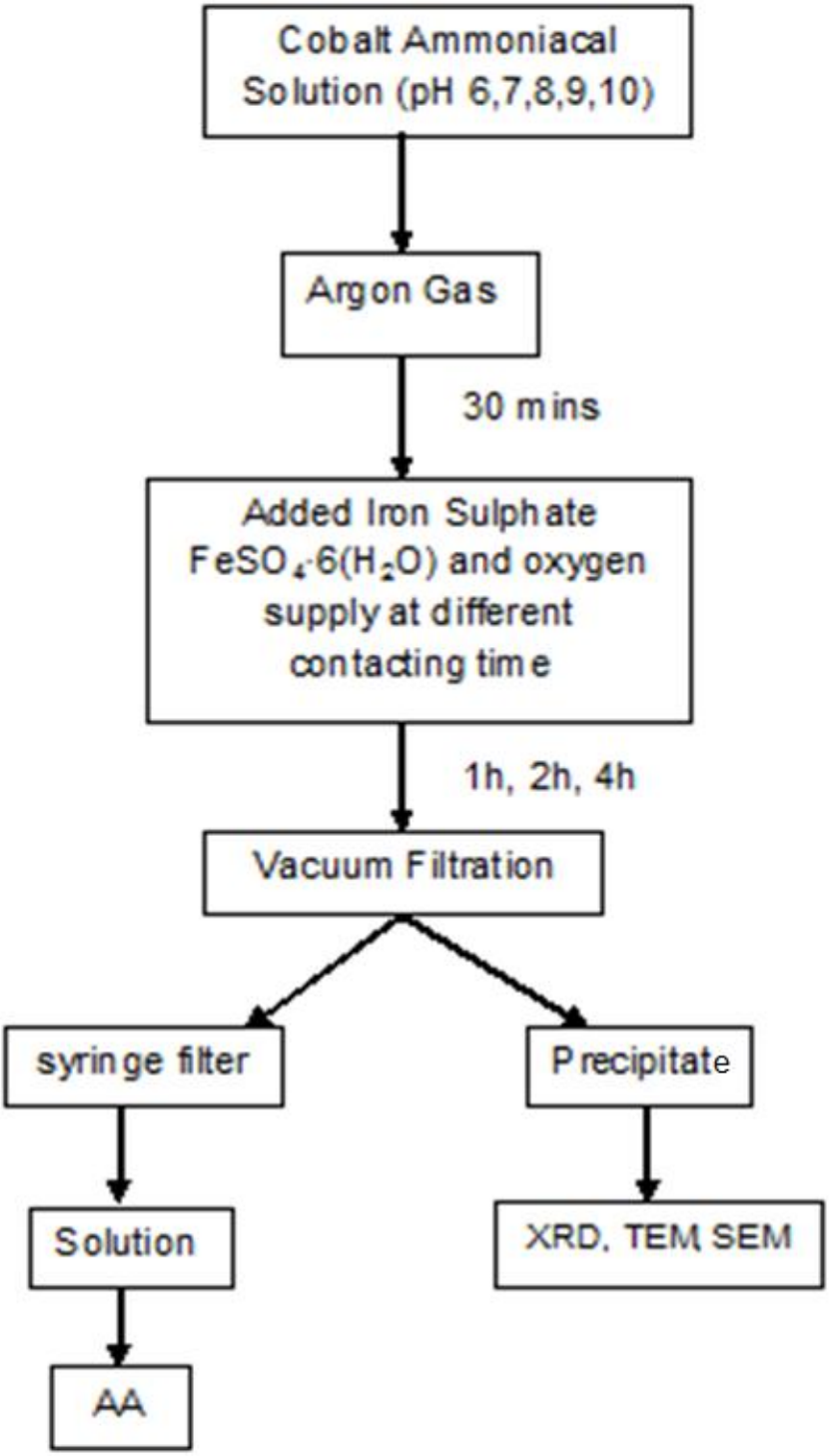

Figure 4.1: The flowsheet of co-precipitation experiments

4.2 Adsorption

The test solutions were prepared as above except that Co was not added until after Fe had precipitated. The color of the solution was initially dark green after iron was added and then turned to rusty brown as iron precipitated. Once the solution color turned to rusty brown, cobalt sulfate was added to the solution and air sparging continued. The solution was stirred for another 90 minutes after cobalt sulfate was added. A sample of the test solution was then gathered as described above. The pH and temperature control were affected by the same methods as for the co-precipitation tests.

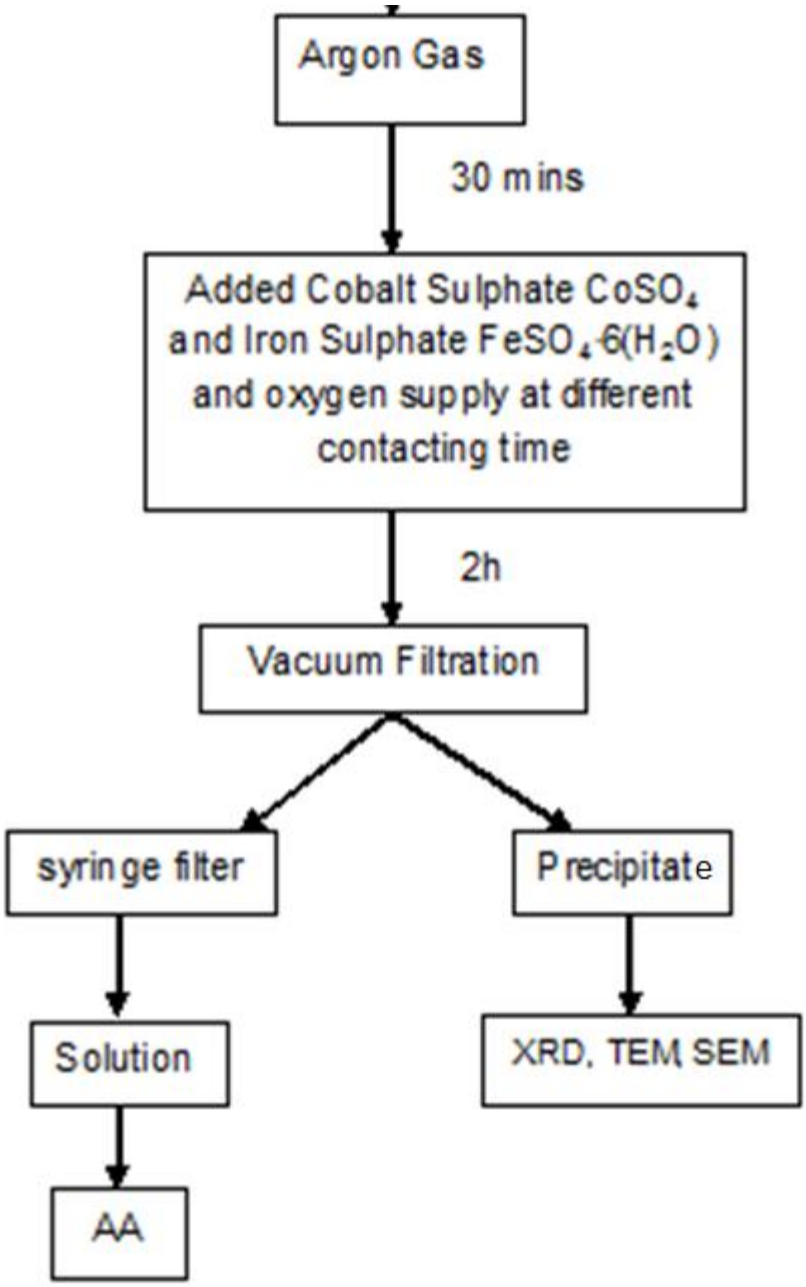

Figure 4.2: The flowsheet of adsorption experiments

4.3 Analysis

For flame atomic adsorption (FAA) analysis, cobalt standard solutions were prepared at 7.5 $mg \cdot L^{-1}$, 5 $mg \cdot L^{-1}$, 2.5 $mg \cdot L^{-1}$, 1 $mg \cdot L^{-1}$, and blank. The cobalt bearing test solutions were diluted 100 times in order to obtain an accurate measurement through FAA.

XRD was used to analyze both the unwashed and washed precipitates. The precipitates were washed with distilled water, dried at 40ºC for 24 h and analysed by XRD. These were ground prior to analysis using a mortar and pestle. The sample was scanned from 10 to 90 degree at a rate of 1 minute per two degree. The voltage for X-ray was 40kV at 20 mA and the X-Ray source was Cu.

SEM was used to analyze both the unwashed and washed precipitates. The precipitates were washed with distilled water, dried at 40ºC for 24 h and analysed by SEM. The precipitates were ground prior to mounting.

TEM was used to analyze some precipitates. The precipitates were washed with alcohol and mounted on the sample holder.

5. RESULTS AND DISCUSSION

5.1 Effect of Iron Concentration

After iron was added to the cobalt solution, it was initially redish and turned dark brown after approximately one hour. This change in colour depended on the iron concentration. After 5, 10 and 20 minutes, the solution of iron sulfate concentrations of 0.1M 0.15M and 0.2 M in cobalt-iron solution turned to lighter brown as shown in Figure 5.1(left). The solution turned to yellowish brown which is shown in Figure 5.1(right) and the precipitate was collected by vacuum filtration (0.45 mm filter paper).

Figure 5.1: (left) Solution of iron sulfate in cobalt-iron solution after 5 minutes; (right) Solution of iron sulfate in cobalt-iron solution after 2 hours

The experimental results show that co-precipitation and adsorption are directly related to iron concentration (Fig. 5.2). As the concentration of Fe increased, the percentage cobalt lost also increased at pH 10. The shape of the cobalt adsorption curve is similar to that obtained by Osseo-Asare and

Fuerstenau (1983). In their work, maximum adsorption on hematite was found at pH 7. The result also shown that as the concentration of iron increased, the cobalt uptake also increased which is coherence with Osseo-Asare and Fuerstenaus' experiment result. Osseo-Asare and Fuerstenau (1987), have also pointed out that the metal lost from solution increased with increased solid-to-liquid ratio implying that the larger amount of adsorbent surface exposed to the metal-bearing ammoniacal solution resulted in more metal lost. Furthermore, this work's experimental results are also generally in agreement with Mehta and Han's (1984) work. From their coprecipitation curve, it can be found that the amount of co-precipitation of cobalt increased with the increased of manganese content in solution. Hence iron concentration is one of the factors, which is responsible for low cobalt recovery. The reason for increasing loss of cobalt with higher dose of adsorbent is that more adsorption sites are available causing higher removal of cobalt. [Borggaard, 1987] The cobalt ions were competing for limiting adsorption sites at lower iron oxide dosage. Also the higher dose of adsorbent provides higher chances for coprecipitation to occur. The difference is coprecipitation is about cobalt that is in grain boundary with iron. Also, as it is shown in Figure 5.2, temperature also affects cobalt adsorption, which will be discussed later in section 5.4 on page 43.

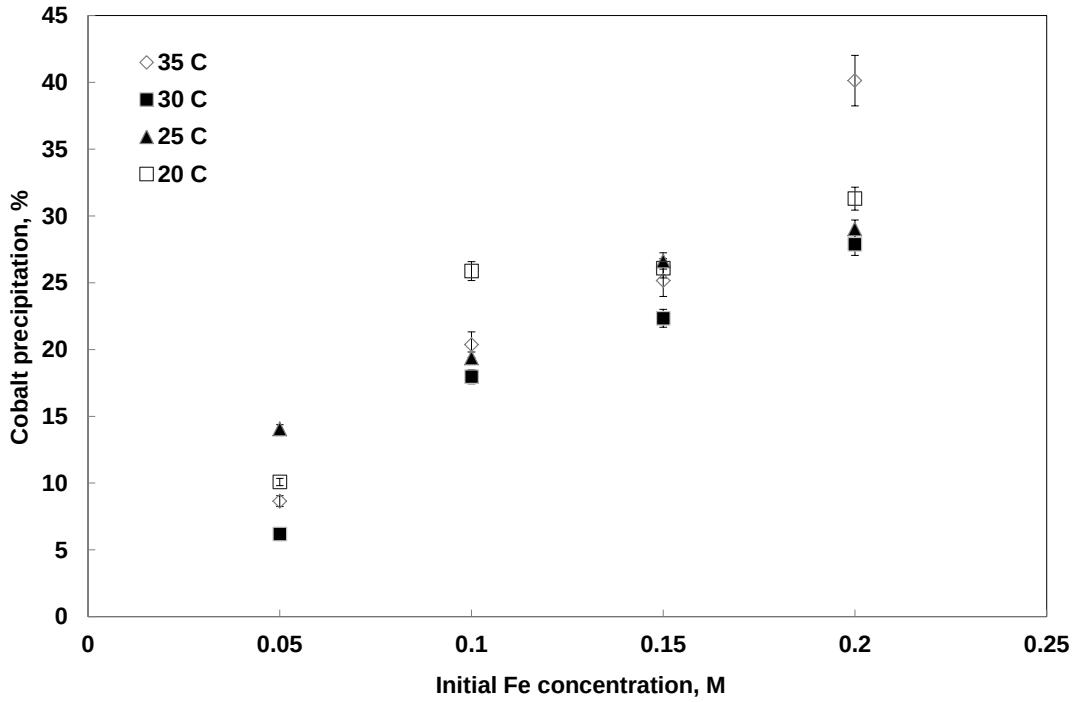

Figure 5.2: Percent cobalt co-precipitated as a function of iron concentration at various temperatures

Throughout these experiments it was important to ensure that all of the ferrous iron was dissolved in the ammoniacal solution prior to precipitation. In Kloche and Hixson's (1972) work, ferrous iron solubility was found to be 0.5 M in 5.49 M total NH_3. [Kloche and Hixson, 1972] In our experiments, the concentrations of iron (II) sulfate used were 0.05 M, 0.1M, 0.15 M and 0.2 M in 6.5 M total ammonia. Thus the ferrous concentration never approached the solubility limit and any precipitate formed during our experiments was the result of oxidation to the ferric state. The percentage of cobalt loss is calculated based on using Flame Atomic Adsorption (FAA) method. During the experiment, cobalt solution was gathered by using syringe filter and then diluted 100 times.

This solution is then tested using FAA with standard cobalt solution; hence the amount of cobalt left in the solution can be known.

5.2 Effect of pH

The effect of pH on the co-precipitation of cobalt and iron over the pH range 6-10 at various iron concentrations was studied and the results are shown in Figure 5.3. It is observed that the percentage of cobalt lost increased with increasing pH up to pH 7, and then decreased up to pH 10. The low cobalt loss at pH 6 indicates that more iron was dissolved and the solubility of iron is approximately $10^{-2.8}$ μ ML^{-1} ; Hence there was less cobalt uptake by iron precipitates. The mass of the precipitates decreased as pH was increased above 7 (Table 5.2). Thus, as could be expected, the amount of cobalt co-precipitated decreased with a decrease in iron precipitate mass. Figure 5.3 shows that to limit cobalt losses by co-precipitation, one should operate the Caron leach at pH close to 10. This is consistent with industry practice. A pH higher than 10 in the leach is avoided to minimize evaporative ammonia losses and reduce the amount of ammonia required in the process. In addition, hydrolysis of ferrous iron can occur at high pH prior to aeration and cobalt/nickel ammines are most thermodynamically stable near pH 10 [Asselin, 2008]. Thus pH is generally maintained just below 10. The reasons for the decrease in mass of precipitate as pH is increased are unclear but it may due to the effect of ionic strength and the addition of sulfuric acid. During the experiment, sulfuric

acid (H_2SO_4) was added to adjust the pH from 10 to 6 gradually with same ammonia concentration. Sulfuric acid will precipitate with ammonia to form ammonia sulphate and this is shown in XRD. The mass of cobalt in the precipitate does not account for the mass change observed in Table 5.2. The lower mass may be due to less structural water or a larger degree of crystallinity associated with the precipitate. Indeed, ferrihydrite is known to transform to crystalline goethite at pH higher than approximately 10 [Maceau and Drits, 1993]. The decreased mass is also related to a decrease in the surface area of the precipitate, which reduces adsorption. For example, the surface area of goethite is considered to be significantly smaller than that of ferrihydrite, which can be as high as 700 cm^2 g^{-1} [Dutrizac and Jambor, 1998]. The color of the filtrates and associated precipitates from selected experiments are shown in (Figure 5.4). The high pH condition resulted in a brown precipitate, which is often associated with goethite or ferrihydrite as well as other iron oxyhydroxides [Dutrizac and Jambor, 1998]. The pH 8 conditions appeared to generate a gelatinous residue of blackish colour. This residue may contain some magnetite, which has been observed under similar conditions [Zuniga et al., 2011]. The colour of the filtrates is unremarkable other than the fact that the pH 6 filtrates were yellowish indicating the presence of soluble iron.

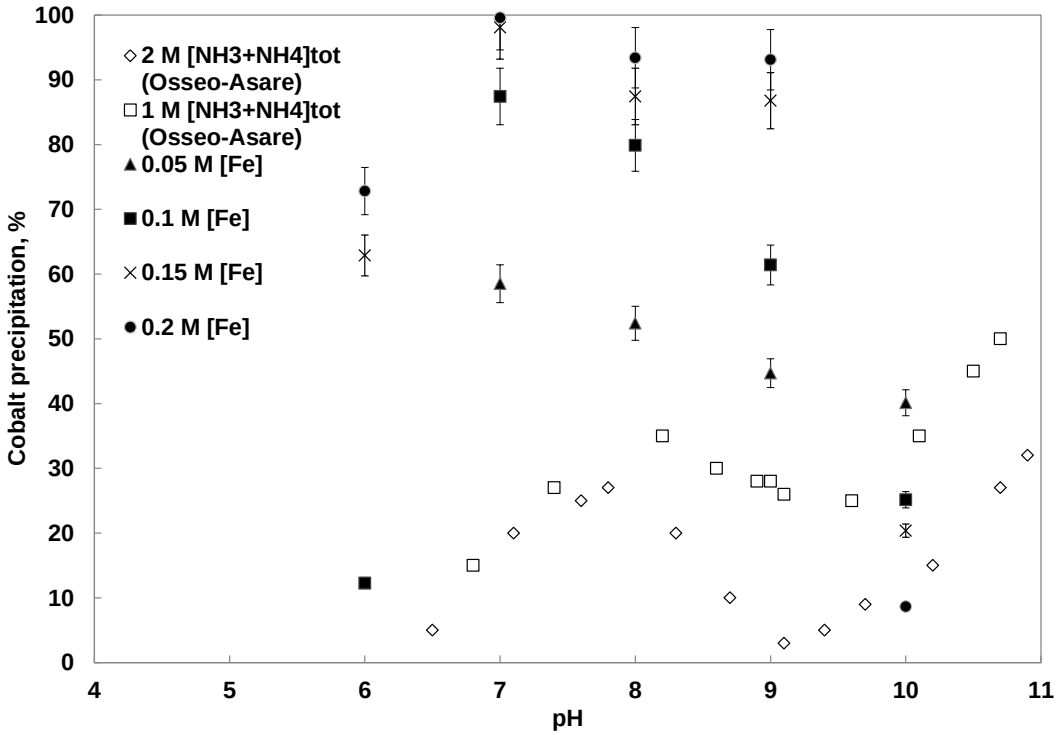

Figure 5.3: Percent of cobalt co-precipitation as a function of pH at various iron concentrations at 35°C with comparison to Osseo-Asare and Fuerstenau's results for adsorption onto hematite (Cobalt [0.001M], Fe [0.0125M] and NH_3 [1.0M])

Table 5.1: Percent cobalt co-precipitation as a function of pH at various initial ferrous concentrations at 35°C and 6.5 M total NH_3

	pH 6	**pH 7**	**pH 8**	**pH 9**	**pH 10**
0.20 M	72.82	99.59	93.41	93.10	40.13
0.15M	62.88	98.08	87.42	86.78	25.15
0.10M	12.70	87.44	79.89	61.41	20.37
0.05M	12.27	58.51	52.41	44.70	8.65

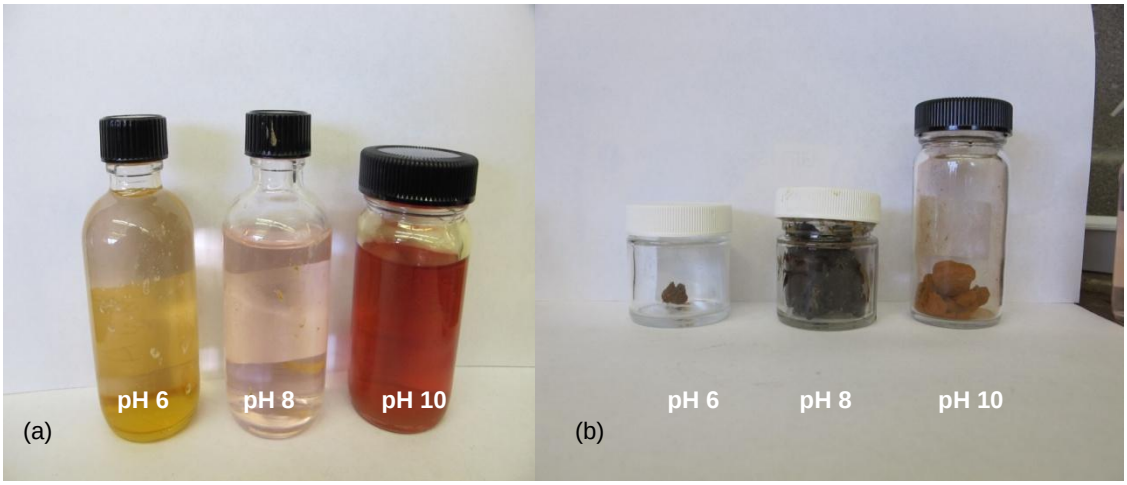

Figure 5.4: (a) Cobalt ammonia filtrates at different pH and $[NH_3]_T$=6.5M (b) Cobalt iron oxide precipitate at different pH at 35°C with 0.15 M Fe for 2 hours and $[NH_3]_T$=6.5M

Table 5.2: Mass of precipitates as a function of pH

pH	Iron Concentration (M)	Precipitate (g)
7	0.2M	11.2
7	0.15M	8.52
7	0.1M	5.28
7	0.05M	1.86
8	0.2M	10.3
8	0.15M	7.86
8	0.1M	4.52
8	0.05M	2.21
9	0.2M	9.89
9	0.15M	6.63
9	0.1M	3.92
9	0.05M	1.84
10	0.2M	4.27
10	0.15M	2.75
10	0.1M	1.67
10	0.05M	0.57

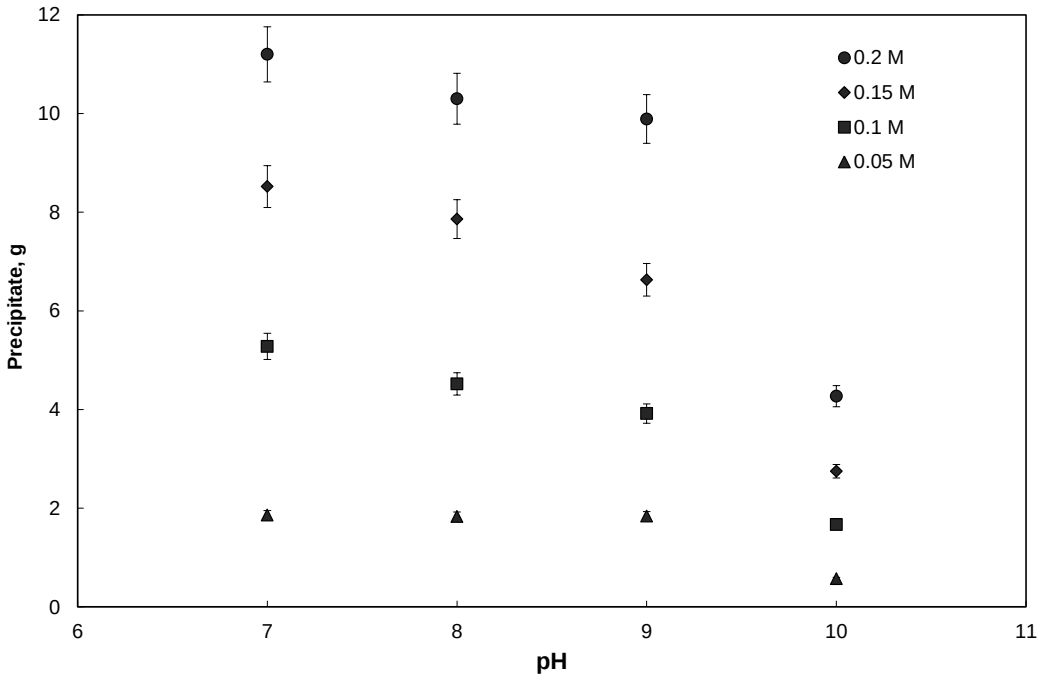

Figure 5.5: Cobalt iron precipitate as a function of pH at various iron concentrations, $[NH_3]_T$ = 6.5M, [Co] = 0.01 M

5.3 Adsorption Experiments

To compare between cobalt adsorption and co-precipitation, a series of percentage cobalt loss experiments was performed as a function of iron concentrations at pH 7 and 35°C as shown in Figure 5.7. Co-precipitation resulted in a higher percentage (~10%) of cobalt loss at every initial iron concentration. The reason is that when iron was in co-precipitation with cobalt, there was also some cobalt being adsorbed on the surface of the iron molecule, which may cause higher amount of cobalt loss. The filtrates as a result of

adsorption and co-precipitation are shown in Figure 5.6. The adsorption condition filtrate shows a darker red color, which is consistent with the higher amount of cobalt in solution.

Figure 5.6: The filtrates of the result of adsorption and co-precipitation at 35°C with 0.15 M Fe for 2 hours at pH 7

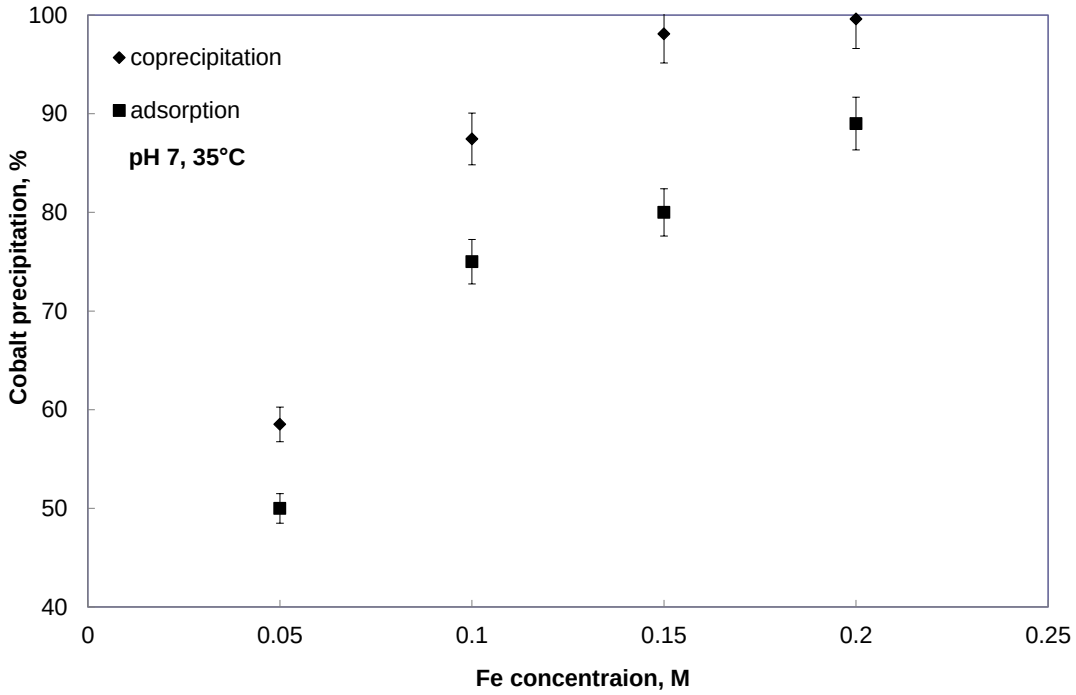

Figure 5.7: The percentage of cobalt loss as a function of various iron concentrations at pH 7

5.4 Effect of Temperature

Figure 5.2 shows the adsorption of cobalt at four different temperatures in 6.5 M NH_3. The influence of temperature is not significant, does not appear to follow a pattern and is largely within the error of measurement between 20 and 35°C. Temperature is known to affect the transformation of amorphous phases of iron such as ferrihydrite to more crystalline phases such as goethite and hematite. The relationship between transformation temperature and solution chemistry is highly complex and difficult to predict, however, transformation

temperatures are generally in the range of 80 to 150°C (Dutrizac and Jambor, 1998 and Loan et al., 2006). Thus, we did not expect to see a strong relationship between cobalt co-precipitation and temperature within the small window tested here.

5.5 Effect of Contacting Time

The rate of cobalt adsorption was determined in 6.5 M NH_3 solution at pH 10 and 25ºC. Figure 5.8 shows that the cobalt adsorption increases steadily with time. This result is similar to that obtained by Osseo-Asare and Fuerstenau (1979). In their work, the percent cobalt adsorption increased up to four hours. At about four hours, the adsorption process reaches equilibrium since all the activation sites are thought occupied. While hydrolysis time is expected to promote transformation of amorphous iron phases to crystalline phases, it appears that the timescales involved in the Caron leach (and tested here) are too short to expect a change in the co-precipitation behavior.

Table 5.3: Percent of cobalt adsorption as a function of contacting time at Fe [0.15M], NH_3 [6.5M], Co [0.01M] with pH 10 and 25°C

Contacting Time	Percentage of Cobalt Loss
1 hour	25.9

Contacting Time	Percentage of Cobalt Loss
2 hours	29.1
4 hours	31.2

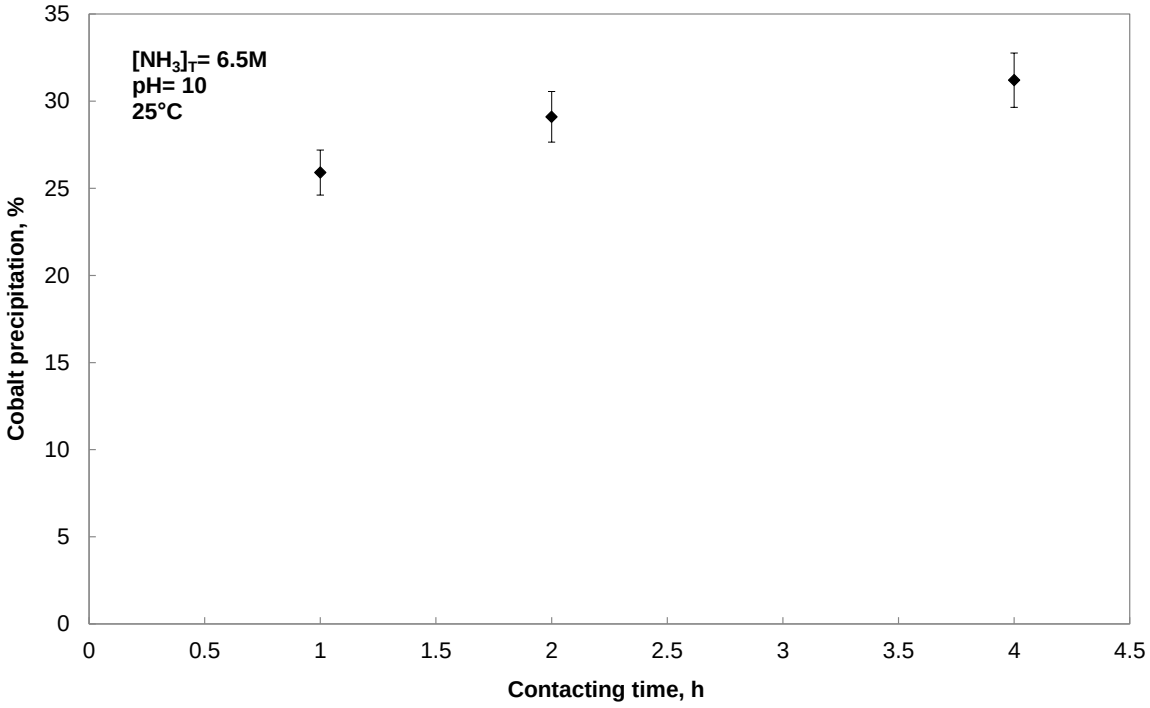

Figure 5.8: Percent of cobalt adsorption as a function of contacting time at pH 10, Fe [0.15M], NH_3 [6.5M], Co [0.01M] and 25°C

5.6 Effect of Total NH_3+NH_4 Concentration

A series of experiments was performed to investigate the effect of the total ammonia concentration on cobalt loss at constant pH. The results are

shown in Figure 5.9. It is found that the amount of co-precipitation decreases as the total ammonia increases from 1.5 M to 6.5 M. As the total ammonia concentration is increased, cobalt loss is decreased due to the increased stability of cobalt ammine complexes. These experiments were performed at pH 10, which is similar to the optimum pH (9.5) suggested by Mehta and Han (1984). Speciation diagrams were calculated using a method developed by Asselin (2008) to demonstrate the effect of total ammonia concentration on cobalt-ammine complex stability. Figures 5.10 and 5.11 show the stability of the various cobalt-ammonia complexes at total ammonia concentrations of 3 and 6.5 M, respectively. Comparison of the two figures clearly shows that larger concentrations of ammonia favour the stability of the hexa-ammine complex. This is evident both by its increased solubility and by its fractional concentration. In short, the findings as regards ammonia concentration are consistent with thermodynamic predictions and industry practice.

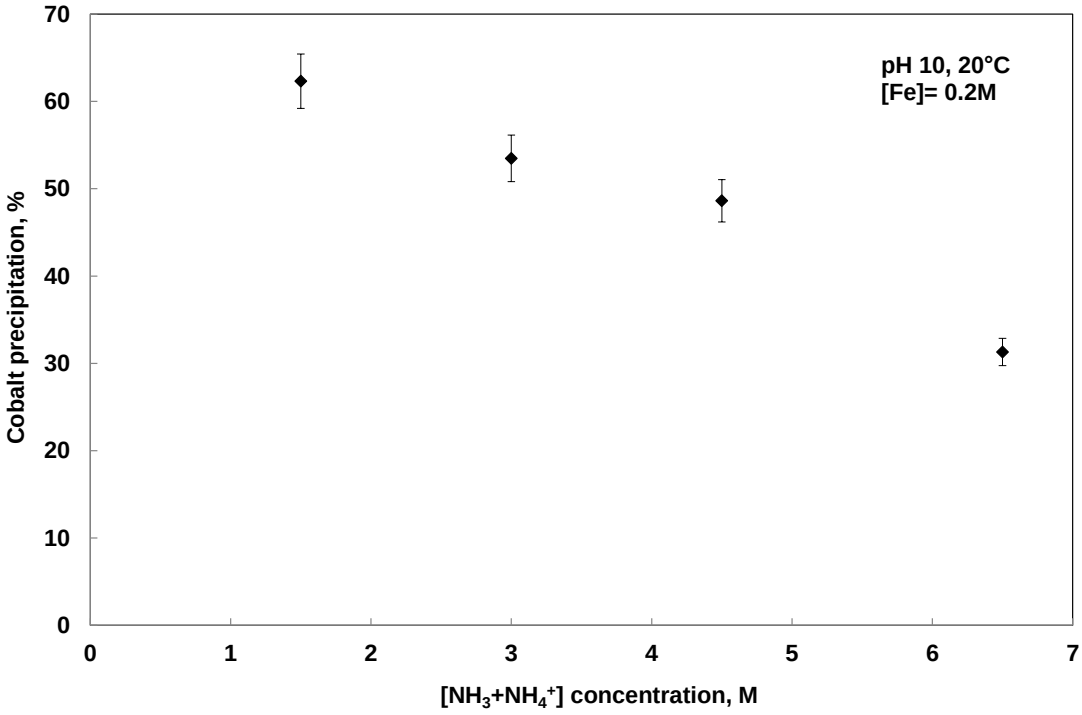

Figure 5.9: Percentage of cobalt loss as a function of total ammonia concentration (NH_3+NH_4) at pH 10, 20°C and 0.2 M of iron

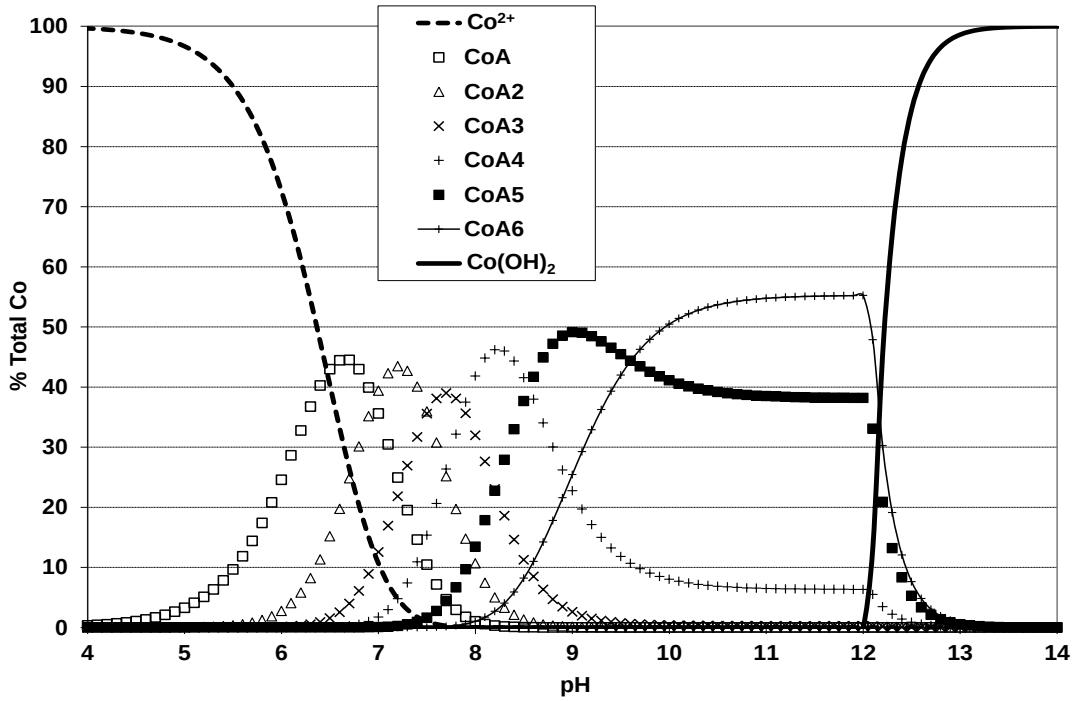

Figure 5.10: Speciation diagram for the Co(II)-NH_3-H_2O system at 25°C. Cobalt concentration is 0.02 M and total ammonia is set to 3 M. "CoAn" represents the ammine species where "n" is the number of ammonia ligands associated with cobalt (from 0 to 6).

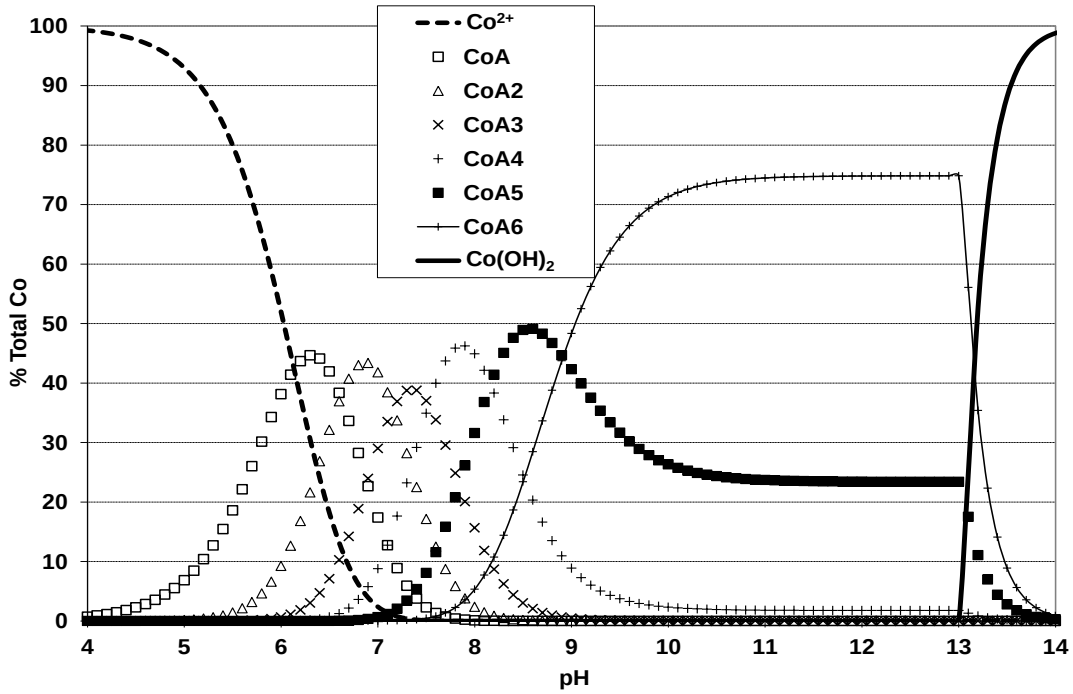

Figure 5.11: Speciation diagram for the Co(II)-NH_3-H_2O system at 25°C. Cobalt concentration is 0.02 M and total ammonia is set to 6.5 M. "CoAn" represents the ammine species where "n" is the number of ammonia ligands associated with cobalt (from 0 to 6).

5.7 Structural Analysis (XRD)

The crystalline phase was identified by X-ray diffractograms. The unwashed and washed precipitate samples contained ammonium sulphate and a low-crystallinity iron phase after tests at pH 8, 9 and 10. The corresponding diffractograms are shown in Figures 5.12, 5.13 and 5.14, respectively. The washed precipitates are characteristic of "2 line" ferrihydrite with peaks matching almost exactly with those seen in Figure 2.4. It appears as though the

co-precipitation/adsorption mechanism is associated with ferrihydrite precipitation, which, whilst being an entirely new finding for the Caron process, is entirely in keeping with the literature on ferric precipitation. It is interesting to note that goethite was not observed in any of the precipitates. At pH 10, given the change in the nature (color) and mass of the precipitates, as observed above, one might have expected to see some crystalline phases present. SEM and EDX showed that iron weight percentage was different at different pH. At higher pH, hydration may occur on the solid. The absence of goethite indicates that the mass changes associated with pH increase may be due to water of hydration changes rather than phase transformation.

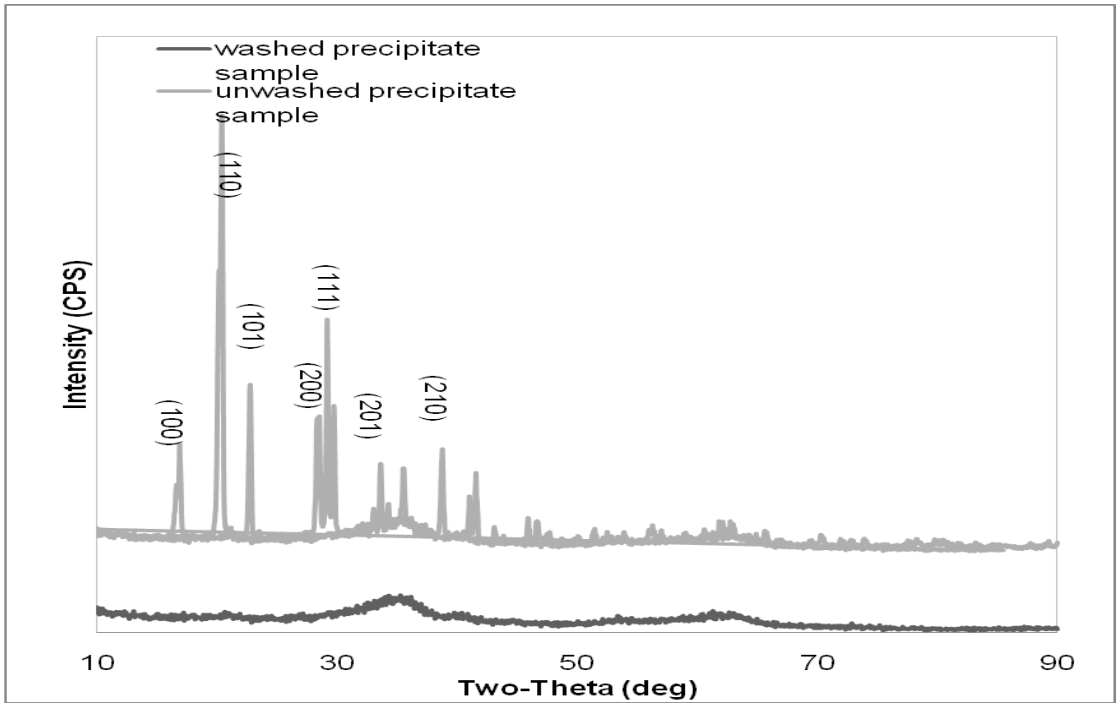

Figure 5.12: XRD pattern of unwashed and washed precipitate samples contain ammonium sulphate and ferrihydrite at pH 8, Fe [0.2M], NH_3 [6.5M], Co [0.01M] and 35^{o}C.

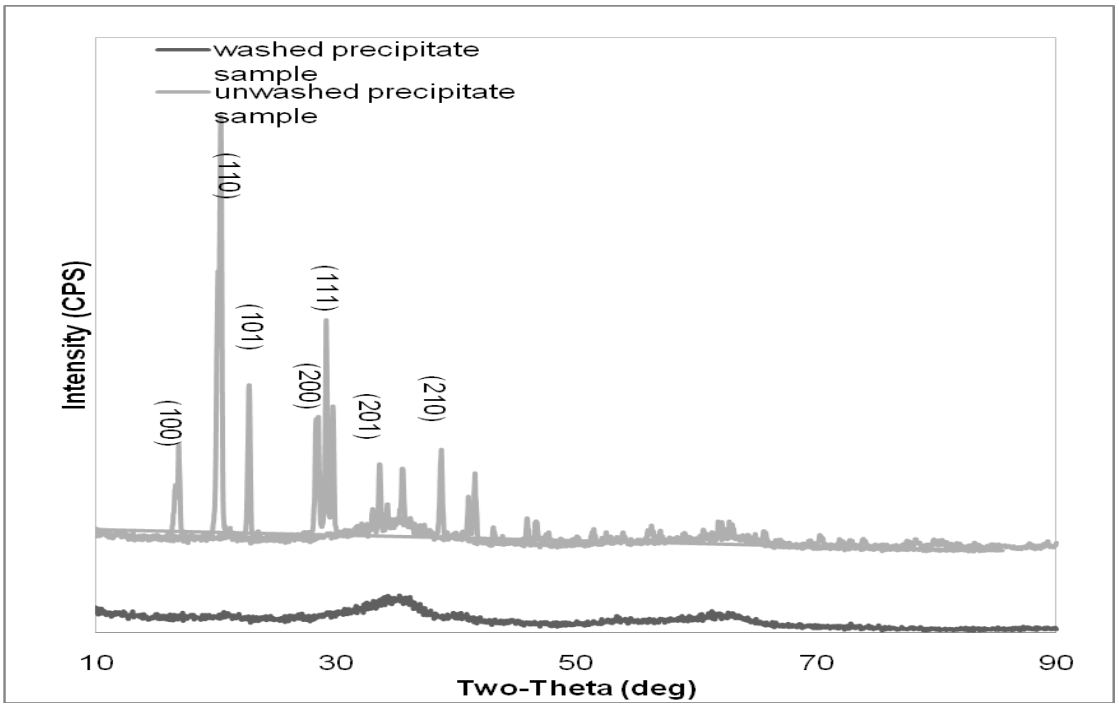

Figure 5.13: XRD pattern of unwashed and washed precipitate samples contain ammonium sulphate and ferrihydrite pH 9, Fe [0.2M], NH_3 [6.5M], Co [0.01M] and 35^{o}C

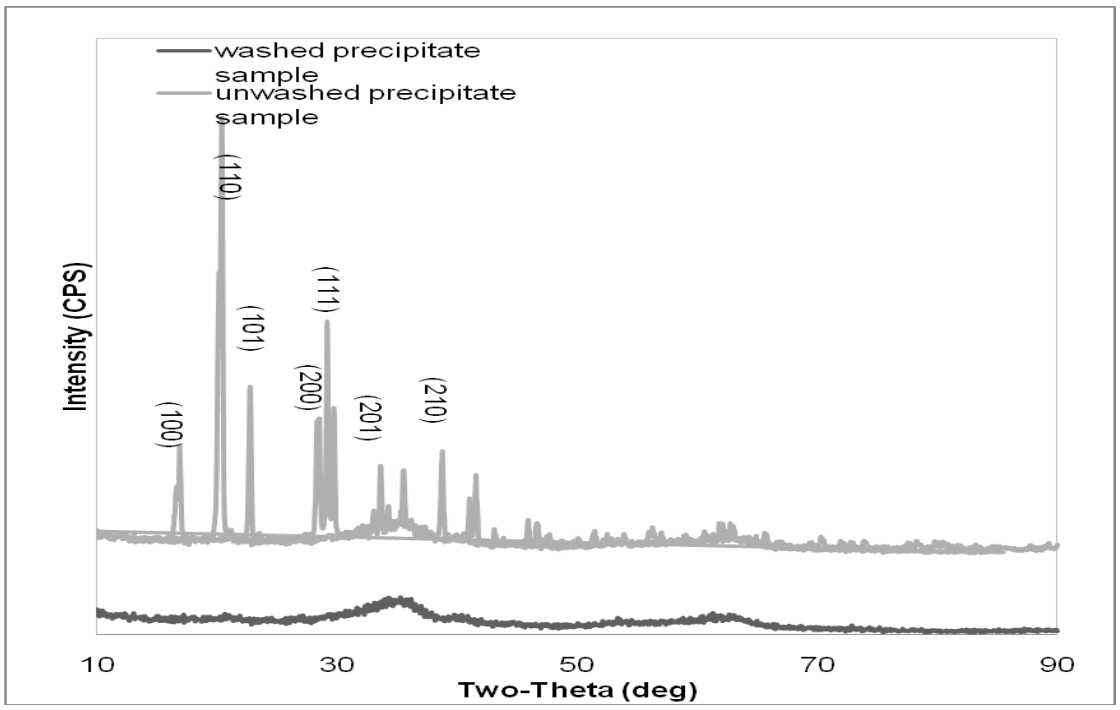

Figure 5.14: XRD pattern of unwashed and washed precipitate samples contain ammonium sulphate and ferrihydrite at pH 10, Fe [0.2M], NH_3 [6.5M], Co [0.01M] and 35^{o}C.

5.8 Microscopy (SEM, EDX)

Selected micrographs are shown in Figures 5.15-5.17. The high-magnification image (Figure 5.16) shows a preponderance of poorly resolved precipitates, which do not appear to be crystalline. The low magnification image of Figure 5.15 shows large particles of roughly 0.5 mm in size consistent with ammonium sulphate crystals. Figure 5.15 is an example of a washed precipitate showing a large amount of small particles. It is difficult to discern any degree of crystallinity from the SEM images obtained. The numbers in the

micrographs shows the points at which EDX spectra were captured and the detailed spectra are presented in Appendix. For the precipitates obtained at various pH and 35°C, figures 5.18 and 5.19 show the iron and cobalt concentrations, as measured by EDX,. Each EDX spectrum showed small traces of cobalt as can be seen from figures A-1 to A-8. The nominal iron to ferrihydrite mass ratio is 58%. From Figure 5.18 it is clear that the precipitates obtained do not have a well-defined molecular formula.

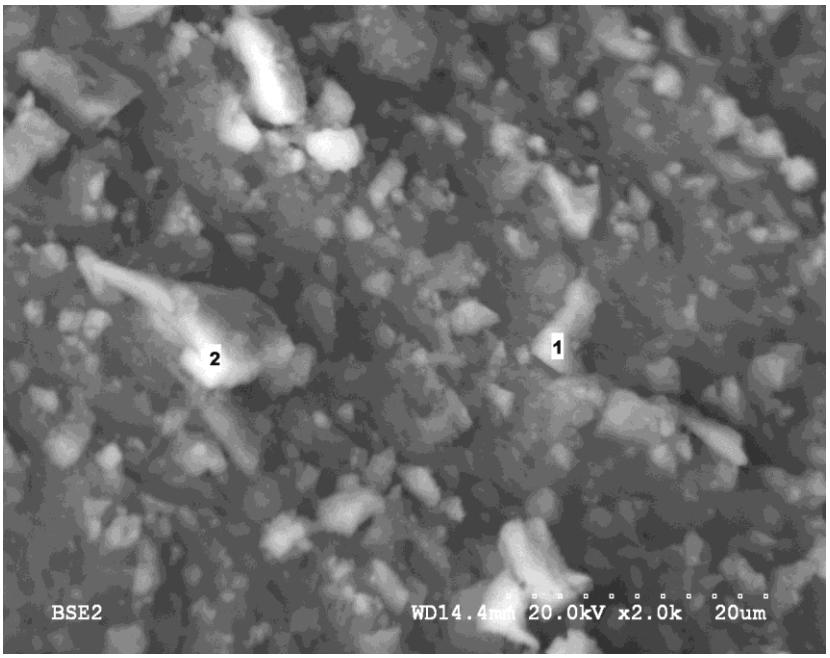

Figure 5.15: SEM photomicrographs of iron oxide precipitate at pH 8, 35ºC, Fe [0.2M], NH_3 [6.5M], Co [0.01M] and 2 hours. This is a washed sample.

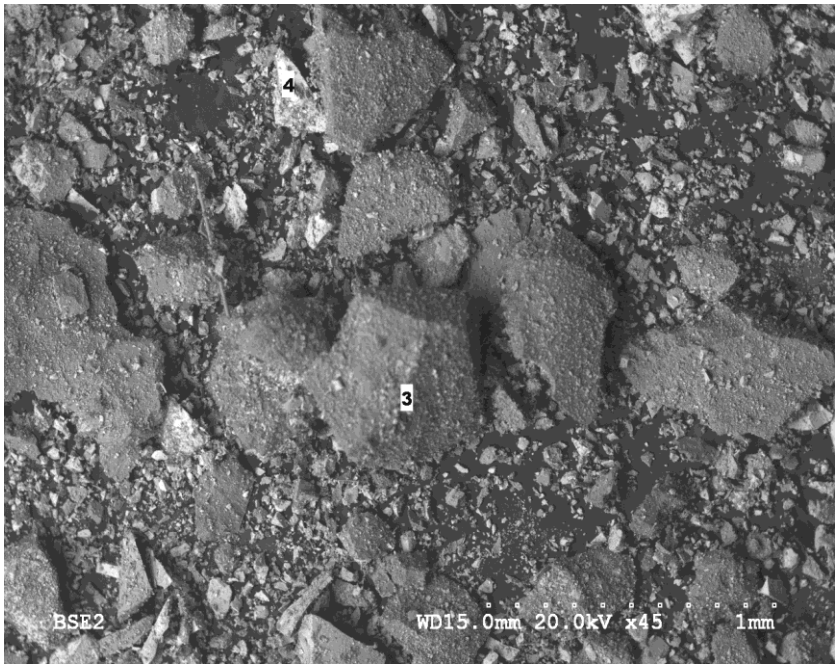

Figure 5.16: SEM photomicrographs of iron oxide precipitate at pH 8, 35ºC, Fe [0.2M], NH_3 [6.5M], Co [0.01M] and 2 hours. This is a non-washed sample.

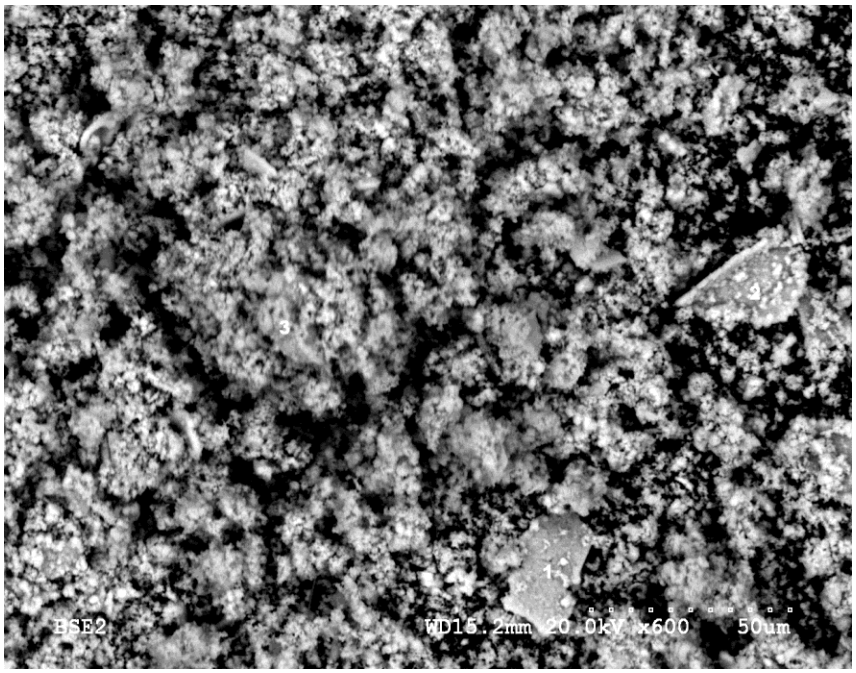

Figure 5.17: SEM photomicrographs of iron oxide precipitate at pH 10, 35ºC, Fe [0.2M], NH_3 [6.5M], Co [0.01M] and 2 hours. This is a non-washed sample.

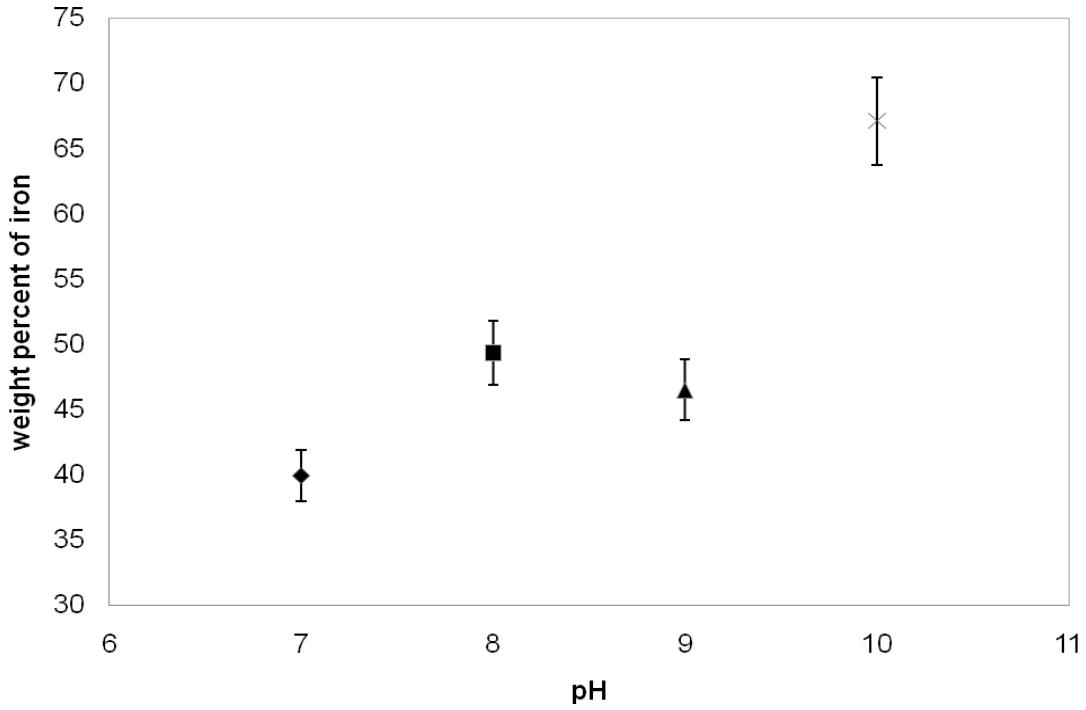

Figure 5.18: Weight percent of iron in different fragments of iron oxide precipitate in pH 7,8,9, and 10.

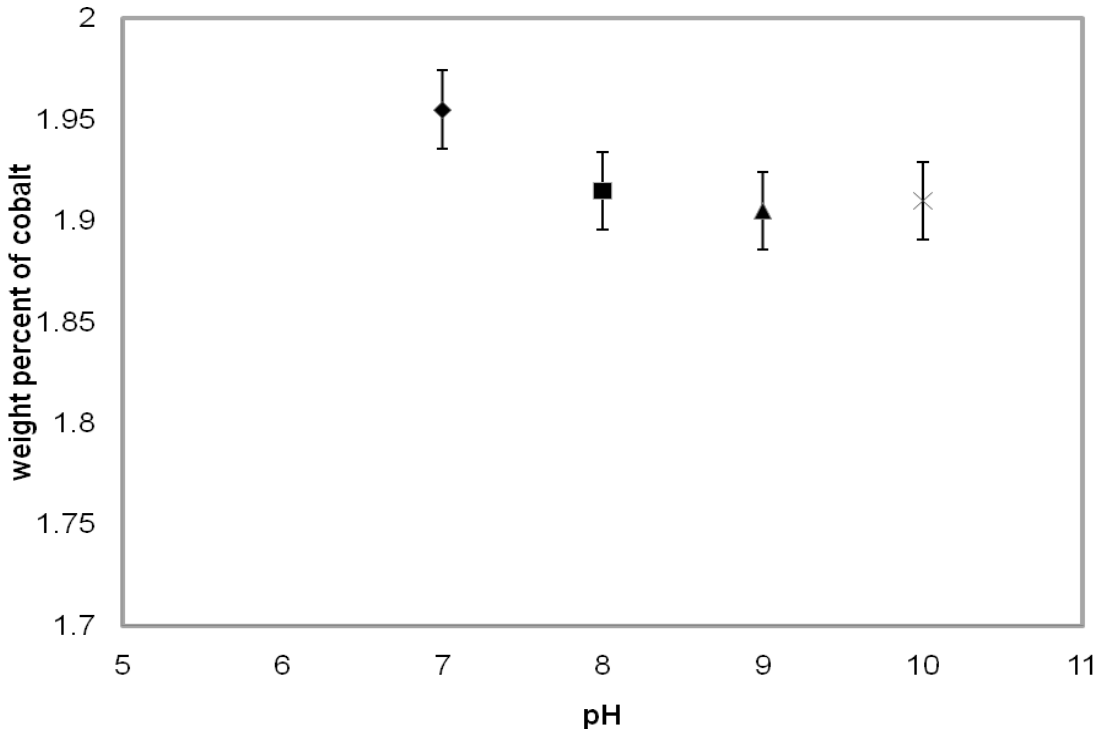

Figure 5.19: Weight percent of cobalt in different fragments of iron oxide precipitate in pH 7,8,9, 10, Fe [0.2M], NH_3 [6.5M], Co [0.01M] and 35^oC

5.9 TEM Analysis

To further clarify the morphology of the cobalt iron precipitates and confirm the adsorption of cobalt by iron oxide, the residue was suspended in the alcohol solution, and then held on a carbon sample support mesh grid. The bright field-imaging mode is the most common mode of operation for TEM analysis. The contrast formation is formed by occlusion and adsorption of electrons directly in the sample. The dark region in the TEM figure indicates a higher atomic number whereas the bright region means no sample in the beam

path. As shown in Figures 5.20-5.23 at different pH values but same iron concentration, since the atomic number of cobalt (A.N. 27) and iron (A.N. 26) are close, TEM cannot clearly distinguish these two atoms. The morphology seen in Figure 5.20 is clearly amorphous and consistent with that observed by other researchers for ferrihydrite (Loan et al., 2006).

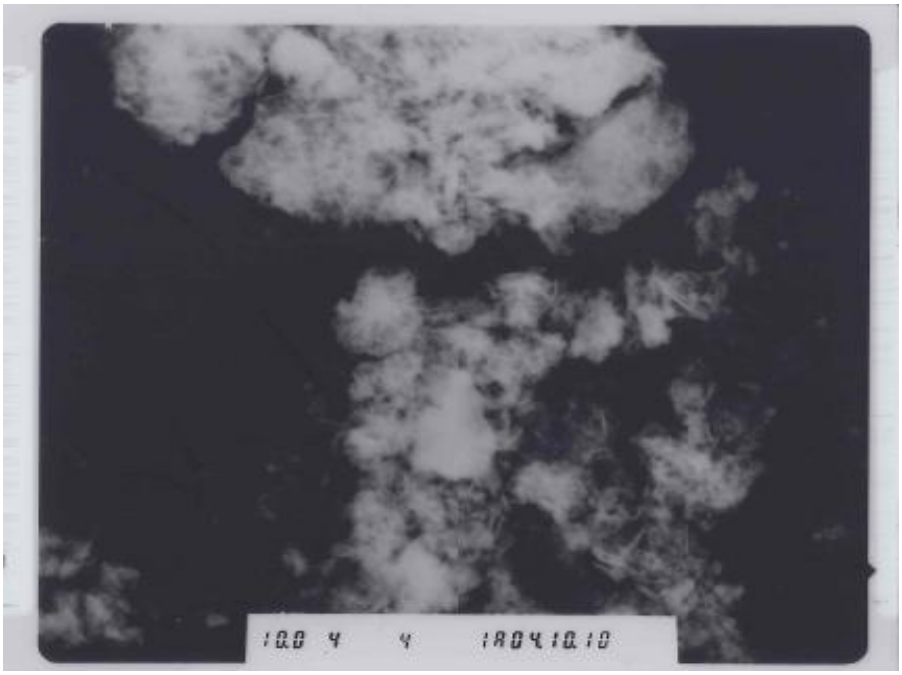

Figure 5.20: Structure characteristics of cobalt iron residue (TEM), pH 7, 0.2 M iron concentration

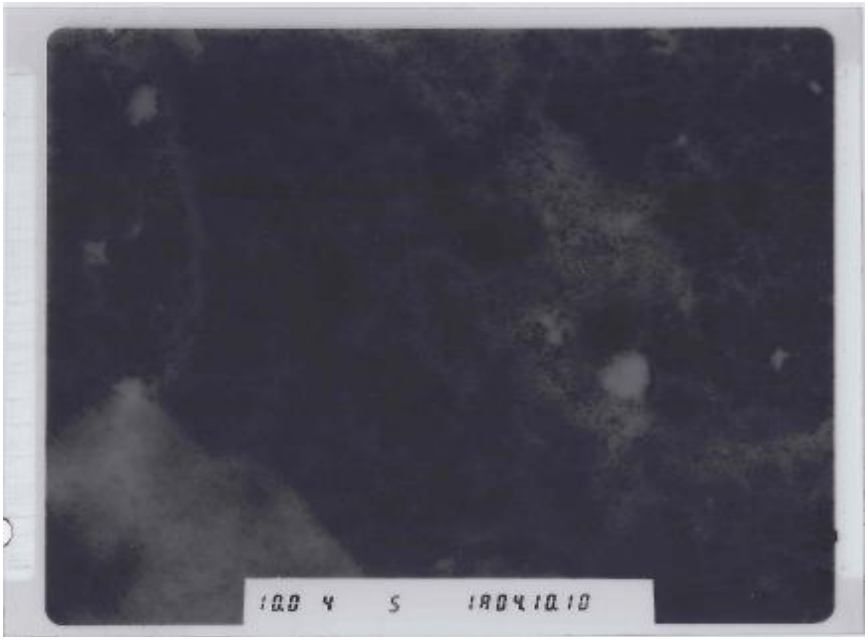

Figure 5.21: Structure characteristics of cobalt iron residue (TEM), pH 8, 0.2 M iron concentration

Figure 5.22: Structure characteristics of cobalt iron residue (TEM), pH 9, 0.2 M iron concentration

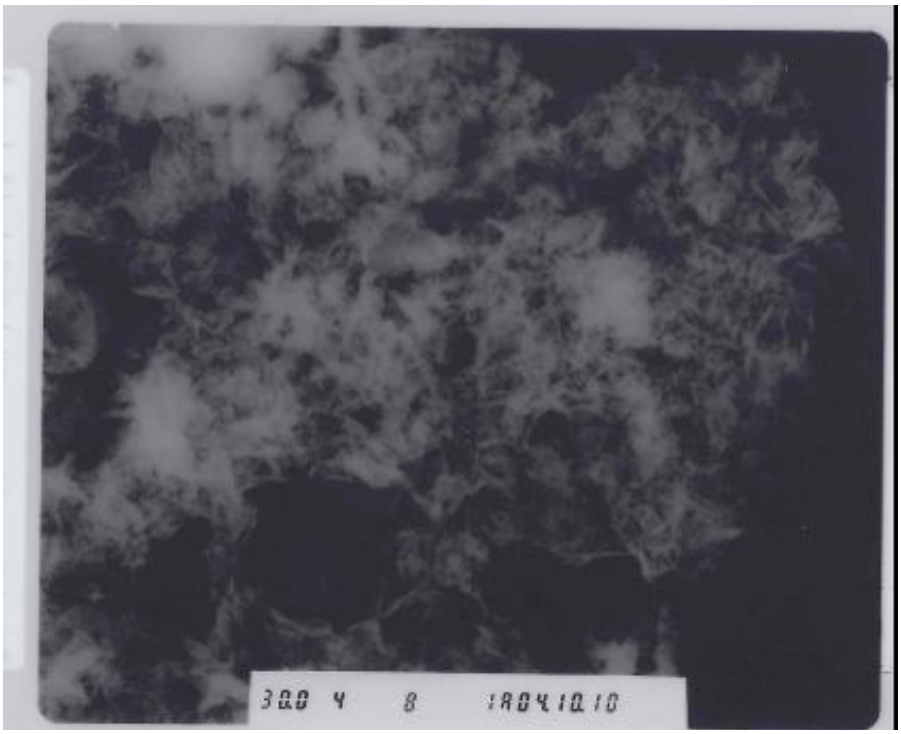

Figure 5.23: Structure characteristics of cobalt iron residue (TEM), pH 10, 0.2 M iron concentration

6. CONCLUSIONS

The low recovery of cobalt in the Caron process is at least partially due to co-precipitation or adsorption onto or with ferrihydrite. Iron concentration can be one of the factors that may affect the cobalt uptake in co-precipitation and adsorption. The concentrations of iron (II) sulfate used were 0.05M, 0.1M, 0.15M and 0.2 M in 6.5 M total ammonia. At pH 10, as the concentration of Fe increased, the percentage cobalt lost also increased. The pH also has a remarkable effect on cobalt uptake since the percentage of cobalt lost increased between pH 6 and 7, then decreased up to pH 10. Co-precipitation, versus adsorption, resulted in a higher percentage (about 10%) of cobalt loss from solution at every initial iron concentration. Moreover, the effect of temperature is not significant, does not appear to follow a pattern, and is largely within the error of measurement between 20 and 35°C. Cobalt adsorption increases steadily with time. As the total ammonia increases from 1.5 M to 6.5 M, the amount of co-precipitation decreases. The washed precipitates which were identified by X-ray diffraction and are characteristic of “2 line” ferrihydrite ($Fe_5HO_8 \cdot 4H_2O$) while goethite was not observed in any of the precipitates. Small amounts of cobalt (~1.9%) were measured in all iron precipitates by EDX. TEM could not clearly distinguish cobalt from iron since their atomic numbers are very similar; however the morphology seen through TEM analysis clearly showed amorphous structures consistent with ferrihydrite.

REFERENCES

Amonette, J.E., and Rai, D., 1990. Identification of noncrystalline (Fe, Cr)(OH)3 by infrared spectroscopy, *The Clay Minerals Society*, 38, 129-136.

Anderson, P.A., Fisher, M., Fittock, J.E., Hultgren, V.M., Jones, E.M., Messenger, R.B., and Moroney, A.S., 2004. Reductive ammoniacal leaching of nickel and cobalt bearing materials, BHP Billiton SSM Technology Pty Ltd, US7601314, WO2004090176.

Angove, M.J., Wells, J.D., and Johnson, B.B., 1999. The Influence of Temperature on the Adsorption of Cadmium (II) and Cobalt (II) on Goethite, *J. of Colloid and Interface Science*, 211, 281-290.

Asselin, E., 2008. Thermochemical aspects of the Fe, Ni & Co-NH3-H2O system relevant to the Caron process. *Hydrometallurgy, 2008*; Proceedings of the Sixth International Symposium. By Courtnery A. Young, Patrick R. Taylor, Corby G. Anderson and Yeonuk Choi, Phoenix, AZ, 522-532.

Borggaard, O.K., 1987. Influence of iron oxides on cobalt adsoroption by soils, *J. Soil Sci*, 38, 229-238.

Boujelben, N., Bouzid, J., Z. Elouear, J., 2009. Adsorption of nickel and copper onto natural iron oxide-coated sand from aqueous solutions: Study of single and binary systems, *J. of Hazardous materials*, 163, 376-382.

Burkin, A.R., 1987. Extractive metallurgy of nickel. Published on behalf of the Society of Chemical Industry by Wiley, New York.

Burzynska, L., Gumowska, W., and Rudnik, E., 2004. Influence of the composition of Cu-Co-Fe alloys on their dissolution in ammoniacal solutions, *Hydrometallurgy,* 71*,* 447-455.

Burzynska, L., Rudnik, E., and Gumowaska, W., 2004. The influence of phase structure on the dissolution of Cu-Co-Fe alloys in sulphuric acid solution and the metals recovery, *Hydrometallurgy*, 71, 447-455.

Byerley, J.J., Rempel, G.L., and Garrido, G.F., 1979. Copper catalyzed leaching of magnetite in aqueous sulfur dioxide, *Hydrometallurgy,* 4, 317-336.

Canterflold, J.H., 1975. Treatment of nickeliferous laterites, *Minerals Science Engineering*, 7, 3-17.

Caron, M.H., 1950. Ammonia Leaching of Nickel and Cobalt Ores, *Transactions Aime, Journal of Metals,* 188, 67-90.

Caron, M.H., 1905. Separation of Nickel and Cobalt, *Transaction Alme, Journal of Metals,* 188, 91-103.

Chander, S., and Sharma, V.N., 1981. Reduction Roasting/ammonia Leaching of Nickeliferous Laterites, *Hydrometallurgy,* 7, 315-327.

Chang, Y.F., Zhai, X.J., Li, B.C., and Fu, Y., 2010. Removal of iron from acidic leach liquor of lateritic nickel ore by goethite precipitate, *Hydrometallurgy,* 101, 84-87.

Chang, Y.C., and Chen, D.H., 2006. Recovery of gold(III) ions by a chitosan-coated magnetic nano-adsorbent, *Gold Bulletin (London, United Kingdom)*, 39, 98-102.

Chiu, H.S., and Wang, J.J., 2009. Adsorption Thermodynamics of Cobalt Ions onto Attapulgite, *Journal of environmental protection science,* 3, 102-106.

Clark, S.J., Donaldson, J.D., and Khan, Z.I., 1996. Heavy metals in the environment. Part VI: Recovery of cobalt values from spent cobalt/manganese bromide oxidation catalysts, *Hydrometallurgy,* 40, 381-392.

Coto, O., Galizia, F., Hernandez, I., Marrero, J., and Donati, E., 2008. Cobalt and nickel recoveries from laterite tailings by organic and inorganic bio-acids, *Hydrometallurgy,* 94, 18-22.

Crawford, R.J., Mainwaring, D.E., and Harding, I. H., 1993. Adsorption and coprecipitation of multiple heavy metal ions onto the hydrated oxides of iron and chromium. *Langmuir*, 9 (11), 3057-62.

Crawford, R.J., Mainwaring, D.E., and Harding, I. H., 1997. Adsorption and coprecipitation of heavy metals from ammoniacal solutions using hydrous metal oxides, *Colloids and surfaces*, 126, 167-179.

Dalvi, A.D., Bacon, W.G., and Osborne, R.C., 2004. Past and future of nickel laterite projects. *Trade Show and Investors Exchange, International Nickel Laterite Symposium TMS 2004-133rd Annual Meeting and Exhibition,* Charlotte, N. Carolina.

Das, R.P., and Anand, S., 1995. Precipitation of iron oxides from ammonia-ammonium sulphate solutions, *Hydrometallurgy*, 38, 161-173.

Davis, J.A., and Leckie, J.O., 1978. Effect of adsorbed complexing ligands on trace metal uptake by hydrous oxides, *Environ. Sci. Technol.* 12, 1309.

Degraaf, J.E., 1979. The treatment of lateritic nickel ores – A future study of the Caron process and other possible improvements; PART I. Effect of Reduction Conditions, *Hydrometallurgy,* 5, 47-65.

Degraaf, J.E., 1980. The treatment of lateritic nickel ores – a further study of the caron process and other possible improvements. PART II. Leaching studies, *Hydrometallurgy,* 5, 255-271.

Dong, D.M., Hua, X.Y., Li, Y., Zhang, J., and Yan, D., 2003. Cd Adsorption Properties of Components in Different Freshwater Surface Coatings: The Important Role of Ferromanganese Oxides, *Environ. Sci. Technol.*, 37*,* 4106-4112.

Dong, D.M., Nelson, Y.M., Lion, L.W., Shuler, M.L., and Chiorse, W.C., 1999. Adsorption of Pb and Cd onto metal oxides and organic material in natural surface coatings as determined by selective extractions: new evidence for the importance of Mn and Fe oxides, *Water Res.,* 34, 427-436.

Dong, D., Liu, L., Hua, X., and Lu, Y., 2007. Comparison of lead, cadmium, copper and cobalt adsorption onto metal oxides and organic materials in natural surface coatings, *Microchemical Journal*, 85, 270-275.

Duncan, P.H., 1985. Trace Metal Adsorption/Coprecipitation on Hydrous Ferric Oxide Under Realistic Conditions, *Water Res*, 10, 1229-1236.

Dutrizac, J.E., Jambor, J.L., 1998. Occurrence and Constitution of Natural and Synthetic Ferrihydrite, a Widespread Iron Oxyhydroxie, *Chemical Reviews,* 98, 2549-2585.

Dutrizac, J.E., Zinck, J.M., 1998. The Behavior of Zinc, Cadmium, Thallium, Tin and Selenium during Ferrihydrite Precipiation from Sulphate Solutions, *CIM Bulletin*, 91, 94-101.

Duval, J.E., and Kurbatov, M.H., 1952. The adsorption of cobalt and barium ions by hydrous ferric oxide at equilibrium, *Journal of Physical* Chemistry, 56, 982.

Fischmann, A. J., and Dixon, D. G., 2009. Awaruite (Ni_3Fe) as a nickel resource- leaching with ammoniacal-ammonium solution containing citrate and thiosulfate, *Hydrometallurgy,* 99, 214-224.

Francis, B., and Reid, J., 2003. Process for nickel and cobalt extraction from laterite ores, *European Patent Specification*, AU2003900387.

Grinstead, R.R., 1984. Selective absorption of copper, nickel, cobalt and other transition metal ions from sulfuric acid solutions with the chelating ion exchange resin XFS 4195, *Hydrometallurgy,* 12, 387-400.

Guo, X.Y., Li, D., Park, K.H., Tian, Q.H., and Wu, Z., 2009. Leaching behavior of metals from a limonitic nickel laterite using a sulfation-roasting-leaching process, *Hydrometallurgy,* 99, 144-150

Habashi, F., 1987*One hundred years of cyanidation, Can. Inst. Min. Metall*., 80, 108-114.

Habashi, F., 1993. *A Textbook of Hydrometallurgy*, 2nd Ed, Quebec.

Habashi, F., 2005. A short history of hydrometallurgy, *Hydrometallurgy*, 79, 15-22.

Han, K.N., Narita, E., and Lawson, F., 1982. The coprecipitation behavior of cobalt (II) and nickel (II) with iron (III), chromium (III), and aluminum (III) from aqueous ammoniacal solutions, *Hydrometallurgy,* 8, 365-377.

Han, K.N., Hoover, M.P., and Fuerstenau, D.W., 1974. Ammonia-ammonium leaching of deep-sea manganese nodules, *Int, J. Min. Proc.,* 1*,* 215-230.

Harvey, R., Hannah, R., and Vaughan, J., 2011. Selective precipitation of mixed nickel-cobalt hydroxide, *Hydrometallurgy*, 105, 222-228.

Isaev, I.D., Tverdokhlebov, S.V., Novikov, L.K., Padar, T.G., Pashkov, G.L., and Mironov, V.E., 1990. The formation of iron(II) ammines in aqueous solution, *Russian Journal of Inorganic Chemistry*, 35 (8), 1162-1164.

James, R.O., and Healy, T.W., 1972. Adsorption of hydrolysable metal ions at the oxide-water interface. II. Charge reversal of silicon dioxide and titanium dioxide colloids by adsorbed cobalt (II), lanthanum (III), and thorium (IV) as model systems, J. *Colloid Interface Sci.*, 40, 53-64.

Jandova, J., and Pedlik, M., 1994. Leaching behavior of iron-nickel alloys in ammoniacal solution, *Hydrometallurgy,* 35, 123-128.

Johnson, B.B., 1990. Effect of pH, temperature, and concentration on the adsorption of cadmium on goethite, *Environ. Sci. Technol.* 24, 112-118.

Kasherininov, G.O., 1960. Behavior of Iron in Ammoniacal Solutions During Leaching of Coblat from its Ores, *J. Appld. Chem*. USSR, 33, 1225-1230.

Kim, H.S., Kho. Y.T., Osseo-Asare, K. Pickering, H.W., 1992. Anodic behaviour of iron in ammoniacal carbonate solutions. *Journal of Electrochemical Society*, 139, 32-39.

Kloche, D. J., and Hixson, A.N., 1972. Solubility of Ferrous Iron in Aqueous Ammoniacal Solutions, *Industrial & Engineering Chemistry Process Design and Development* ,11(1), 141-146.

Kumar, R., Ray, R.K., and Biswas, A.K., 1983. Physicochemical nature and leaching behavior of goethites containing nickel, cobalt, and copper in the sorption and coprecipitation mode, *Hydrometallurgy*, 25, 61-83

Landry, C.J., Koretsky, C.M., Lund, T.J., Melinda, S., and Das. S., 2009. Surface complexation modeling of Co(II) adsorption on mixtures of hydrous ferric oxide, quartz and kaolinite, *Geochimica et Cosmochimica Acta*, 73, 3723-3737.

Lee, H.Y., Kim, S.G., and Oh, J.K., 2005. Electrochemical leaching of nickel from low-grade laterites, *Hydrometallurgy*, 77(3-4), 263-268.

Li, J.H., Li, X.H., Hu, Q.Y., Wang, Z.X., Zhou, Y.Y., and Zhang, J.C., 2009. Effect of pre-roasting on leaching of laterite, *Hydrometallurgy,* 99, 84-88.

Liu, K., Chen, Q. and Hu, H., 2009. Comparative leaching of minerals by sulfuric acid in a Chinese ferruginous nickel laterite ore, *Hydrometallurgy,* 98, 281-286.

Liu, H.Y., and Hernanez, O.Y.C., 2009. Process for the recovery of nickel and/or cobalt from high ferrous content laterite ores, *PCT Int. Appl.* WO 2009114903 A1 20090924.

Loan, M., Newman, O.M.G., Farrow, J.B., and Parkinson, G.M., 2006. Continuous Reactive Crystallization of Nanoscale Six-Line Ferrihydrite, *Crystal Growth & Design,* 6(1), 79-86.

Manceau, A., and Drits, V.A., 1993. Local structure of ferrihydrite and feroxyhite by EXAFS spectroscopy. *Clay Miner*, 28, 165-184.

Means, J.L., Caerar, D.A., and Borcsik, M.P., 1978. Adsorption of Co and selected actinides by Mn and Fe oxides in soils and sediments, *Geochimica et Cosmochimica Acta*, 42, 1763-1773.

Mehta, R.K., and Han, K.N., 1984. The selective removal of cobalt (II) from nickel (II) by coprecipitation with manganese in ammoniacal solutions, *International Journal of Mineral Processing*, 13, 297-312.

Mohapatra, M., Anand, S., Das, R.P., Upadhyay, Chandan., and Verma, H.C., 2002. Preparation and characterization of Cu(II), Ni(II) or Co(II) ion-doped goethite samples and their conversion to magnetite in NH_3-$FeSO_4$-H_2O medium, *Hydrometallurgy*, 66, 125-134.

Moskalyk, R.R., and Alfantazi, A.M., 2002. Nickel lateriate processing and electrowinning practice, *Minerals Engineering*, 15*,* 593-605.

Muir, D.M., Parker, A.J.,Filmer, A.O., Wadley, L.G.B., and Clare, B.W., 1981. Formation of Sulfur from the Ammonia/Oxygen Leach of Copper and Nickel Sulfides. In: Proceedings of Hydrometallurgy' 81, Manchester, UK. Society of Chemical Industry, B3/1-B3/14.

Muir, D.M., and Ho, E., 2006. Process review and electrochemistry of nickel sulphides and nickel mattes in acidic sulphate and chloride media. *Transactions of the Institution of Mining and Metallurgy 115C*, 27-65.

Mustafa, S., Tasleem, S., Naeem, A., and Safdar, M., 2008. Solvent effect on the electrophoretic mobility and adsorption of Cu on iron oxide, *Colloids and Surfaces A: Physicochem. Eng. Aspects*, 330, 8-13.

Nam, C.W., Kim, B.S., and Park, K.H., Recovery of cobalt, nickel and coopper from manganese nodules by reduction roasting and smelting*, The Korean Society for Geosystem Engineering*, 40, 191-197.

Nelson, Y.M., Lion, L.W., Shuler, M.L., and Ghiorse, W.C., 2002. Effect of oxide formation mechanisms on lead adsorption by biogenic manganese (hydr)oxides, iron (hydr)oxides, and their mixtures. *Environ Sci Technol*, 36, 421-425.

Nicol, M.J., 1975. Electrochemical investigation of copper, nickel, copper-nickel alloys in ammonium carbonate solutions, *Journal of the Southern Institure of Mining and Metallurgy,* 75, 291-302.

Nicol, M.J., Nikoloski, A.N., Fittock, J.E., 2004. A fundamental study of the leaching reactions involved in the Caron process. In: Imrie, W.P., Lane, D.M. (Eds.). International Laterite Symposium, TMS, Warrendale, pp 369-380.

Nicol, M.J., Senaputra, A., and Senanayake, G., 2010. Effect of thiosulfate, sulfide, copper(II), cobalt (II)/(III) and iron oxides on the ammoniacal carbonate leaching of nickel and ferronickel in the Caron process. *Hydrometallurgy*, 105(1-2), 60-68.

Nikoloski, A.N., 2002. The electrochemistry of the leaching of pre-reduced nickel laterites in ammonia/ammonia/ammonium carbonate solutions. Ph.D. Thesis, Murdoch University, Perth, Western Australia.

Nikoloski, A.N., Nicol, M.J., and Fittock, J.E., 2003. *Electrochemistry in mineral and metal processing VI*, *Electrochemistry Society Proceedings*, 18, 205-218.

Nikoloski, A.N., and Nicol, M.J., 2006. The electrochemistry of the leaching reactions in the Caron Process. I. Anodic Processes, *ECS Transactions*, 2(3), 197-207

O'Connor, F., Cheung, W.H., Valix, M., 2006. Reduction roasting of limonite ores: effect of dehydroxylation, *International Journal of Mineral Processing*, 88(2-4), 88-99.

Olanipekun, E.O., 2000. Kinetic of leaching laterite, *Int, J. Miner. Process*, 60, 9-14.

Osseo-Asare, K., 1981. Application of activity-activity diagrams to ammonia hydrometallurgy: 2-Fe-NH_3-H_2O, Fe-NH_3-H_2O-CO_3 and Fe-NH_3-H_2O-SO_4 systems at 25°C. *Transactions of the Institution of Mining and Metallurgy,* 90C, 159-163.

Osseo-Asare, K., and Fuerstenau, D.W., 1978. Adsorption losses in ammonia leaching of copper, nickel and cobalt from deep-sea manganese nodules*,* In: *M. J. Jones* (Ed.), Comoplex Metallurgy `78. Institute of Mining and Metallurgy, London, pp. 43-48.

Osseo-Asare, K. and Fuerstenau, D.W., 1979. Adsorption Phenomena in hydrometallurgy, 1. The uptake of Copper, Nickel and Cobaly by Oxide Adsorbents in Aqueous Ammoniacal Solutions. *International Journal Mineral Processing,* 6 (2), 85-104.

Osseo-Asare, K., and Fuerstenau, D.W., 1980. Adsorption Phenomena in Hydrometallurgy III. Model for Copper, Nickel and Cobalt Uptake by Oxide Adsorbents in Aqueous Ammoniacal Solutions, *International Journal Mineral Processing,* 7, 219-234.

Osseo-Asare, K., and Fuerstenau, D.W., 1987. Adsorption of Copper, Nickel, and Cobalt by Oxide Adsorbents from Aqueous Ammoniacal Solutions, *J. Colloid Interface Sci,* 118, 524.

Osseo-Asare, K., Lee, J.W., Kim, H.S., and Pickering, H.W., 1983. Coblat extraction in ammoniacal solution: electrochemical effect of metallic iron. *Metallurgical Transactions B*, 14B, 571-576.

Osseo-Asare, K., and Pickering, H.W., 1983. Cobalt Behavior in Ammonia Leaching Systems, From Report BUMINES-OFR-64-84; Order No. PB84-172295, 30pp.

Park, K.H., Mohapatra, D., Reddy, B.R., and Nam, C.W., 2007. A study on the oxidative ammonia/ammonium sulphate leaching of a complex (Cu-Ni-Co-Fe) matte, *Hydrometallurgy,* 86, 164-171.

Pickles, C.A., 2004. Microwave heating behavior of nickeliferous limonitic laterite ores, *Miner.Eng.* 17, 775-784.

Pardo, F.G., Dempsey, J.P., 1986. Indigenous solid reductants in Caron type nickel plant. *Proceedings Nickel Metallurgy*. Volume I. Extraction and Refining Toronto –CA. Canadian Institute of Mining and Metallurgy, 320-333.

Rademaker, P.D., and Bradbury, J. A., 1979. Ammoniacal Leach of Cobalt from Reduced Lateritic Ores, *J. Metals*, 31(12), 102.

Raghavan, S., and Fuerstenau, D.W., 1975. The adsorption of aqueous octylhydroxamate on ferric oxide, *J. of colloid and Interface Science*, 50, 319-330.

Reid, J., and Barnett, S., 2002. Nickel Laterite Hydrometallurgical Processing Update, Nickel-Cobalt- 8, *Technical Sessions Proceedings,* Alta Metallurgical Services, Perth, W. Australia.

Reid, J.G., and Fittock, J.E., 2004. Yabulu 25 Years On. In: Imrie, W.P., Lane, D. M. (Eds.) Proceeding of International Laterite Nickel Symposium – 2004: 599. TMS. Charlotte- NC.

Robins, R.G., and Huang, J.C.Y., The Adsorption of Arsenate Ion by Ferric Hydroxide, Univeristy of New South Wales Kensington, N.S.W. 2033 Australia.

Rudnik, E., Burzynska, L., and Gumowska, W., 2009. Hydrometallurgical recovery of copper and cobalt from reduction-roasted copper converter slag, *Hydrometallurgy*¸ 22, 85-95.

Saha, A.K., Shahani, M.J., and Altekar, V.A., 1976/1977. Adsorption of Cobalt by Lignite. *Hydrometallurgy,* 2, 285-292.

Scansetti, G., Botta, G.C., Spinelli, P., Reviglione, L., and Ponzetti, C., 1994. Absorption and excretion of cobalt in the hard metal industry, *Science of the Total Environment*, 150, 141-144.

Schwertmann, U., 1991. Solubility and dissolution of iron oxides, *Plant and Soil*, 130, 1-25.

Schwertmann, U., Friedl, J., Stanjek, H., 1999. Fe(III) ions to ferrihydrite and then to hematite. *Journal of Colloid and interface Science,* 209, 215-223.

Schwertmann, U., Cornell, R.M., 1979. Influence of organic anions on the crystallization of ferrihydrite, *Clays and Clay Minerals*, 27(6), 402-10.

Schwertmann, U., Cornell, R.M., 2000. Iron Oxides in the Laboratory. Preparation and Characterisation. *VCH,* Weinheim, 137. DOI: 10.1002/9783527613229.

Sen, T.K., Mahajan, S.P., and Khilar, K.C., 2002. Adsorption of Cu^{2+} and Ni^{2+} on iron oxide and kaolin and its importance on Ni^{2+} transport in porous media, *Colloids and Surfaces A: Physicochem. Eng. Aspects*, 211, 91-102.

Senanayake, G., and Das, G.K., 2004. A comparative study of leaching kinetics of limonitic laterite and synthetic iron oxides in sulfuric acid containing sulfur dioxide, *Hydrometallurgy,* 72, 59-72.

Senaputra, A., Senanayake, G., Nicol, M.J., and Nikoloski, A., 2008. Proceedings of the Sixth International Symposium, *Hydrometallurgy*, 551-559.

Sharma, I.G., Alex, P., Bidaye, A.C., and Suri, A.K., 2005. Electrowinning of cobalt from sulfate solutions, *Hydrometallurgy,* 80, 132-138.

Siemens, R.E., and Corrick, J.D., 1997. Process for recovery of nickel, cobalt, and copper from domestic laterites, *Min. Cong. J.***,** 63, 29-34.

Turner, A., Le Roux, S.M., and Millward, G.E., 2008. Adsorption of cadmium to iron and manganese oxides during estuarine mixing, *Marine Chemistry,* 108, 77-84.

Valant, M., Axelsson, A.K., Aguesse, F., and Alford, N.M., 2010. *Advanced Functional Materials,* 644-647. (Molecular Auxetic Behavior of Epitaxial Co-Ferrite Spinel Thin Film)

Valix, M., and Cheung, W.H., 2002. Study of phase transformation of laterite ores at high temperature, *Minerals Engineering*, 15, 607-612.

Veglio, F., Recinella, M., Massacci, P., and Toro, L., 1994. Screening tests, in the study of iron oxide leaching by sucrose in sulphuric acid solution, using statistical methods, *Hydrometallurgy*, 35, 293-311.

Vol'ska, É., 1979. IR Spectroscopic Investigation of The Aged Products of $Fe(OH)_3$ and $Al_{0.03}Fe_{0.37}(OH)_3$, Institute of Chemistry, A. Mitskevich University, Poznan, Poland, 30(1), 80-83.

Vu, C., and Han, K.N., 1977. Leaching Behavior of Coblat in Ammonia Solutions, Trans. IMM, 86, C119-C125.

Vu, C., Han, K.N., and Lawson, F., 1980. Leaching behavior of cobaltous and cobalto-cobaltic oxides in ammonia and in acid solutions, *Hydrometallurgy,* 6, 75-87.

Wilson, A.R., Lion, L.W., Nelson, Y.M., Shuler, M.L., Ghiorse, W.C., 2001. The Effects of pH and Surface Composition on Pb Adsorption to Natural Freshwater Biofilms, *Environ. Sci. Technol.,* 35, 3182-3189.

Wu, D.B., Zhao, J., Zhang, L., Wu, Q.S., and Yang, Y.H., 2010. Lanthanum adsorption using iron oxide loaded calcium alginate beads, *Hydrometallurgy*, 101, 76-83.

Xavier, F.M.R.S., Ciminelli, V.S.T., 2008. Development of technical and economic parameters affecting process selection to treat nickel laterite ores, In: Young, A. C., Taylor, P.R., Anderson, C.G., Choi. Y. (Eds.), *Hydrometallurgy 2008- 6th International Symposium.* SME, Littleton, pp. 532 -540.

Xu, Y., Axe, L., Boonfueng, T., Tyson, T.A., Trivedi, P., and Pandya, K, 2007. Ni(II) complexation to amorphous hydrous ferric oxide: An X-ray absorption spectroscopy study, *J. of Colloid and Interface Science*, 314, 10-17.

Zuniga, M., Parada L, F., and Asselin, E., 2010. Leaching of a limonitic laterite in ammonia solutions with metallic iron. *Hydrometallurgy*, 104 (2), 260-267.

APPENDIX- EDX SPECTRA IN FRAGMENTS 1 AND 2 IN IRON OXIDE PRECIPITATES

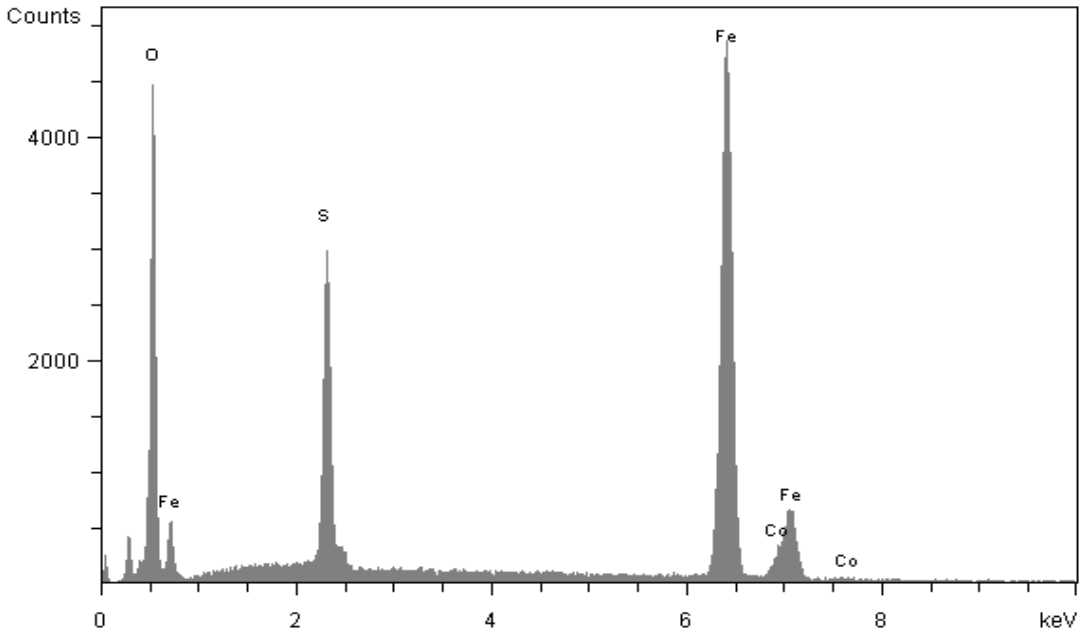

Figure A-1: EDX of each element of fragment 1 in iron oxide precipitate at pH 8, 35ºC, and 2 hours

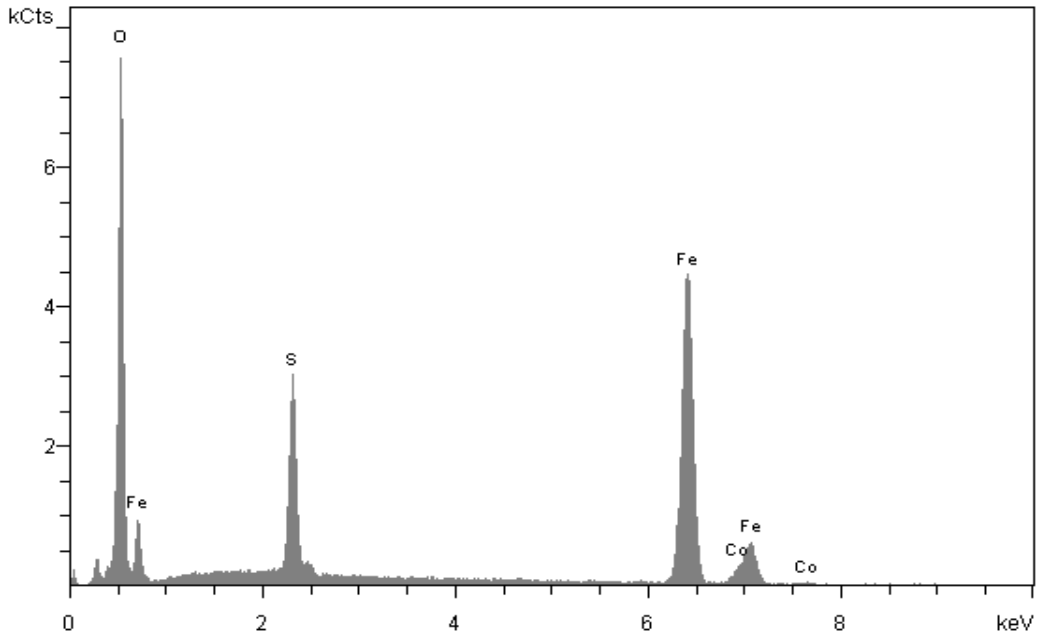

Figure A-2: EDX of each element of fragment 2 in iron oxide precipitate at pH 8, 35ºC, and 2 hours

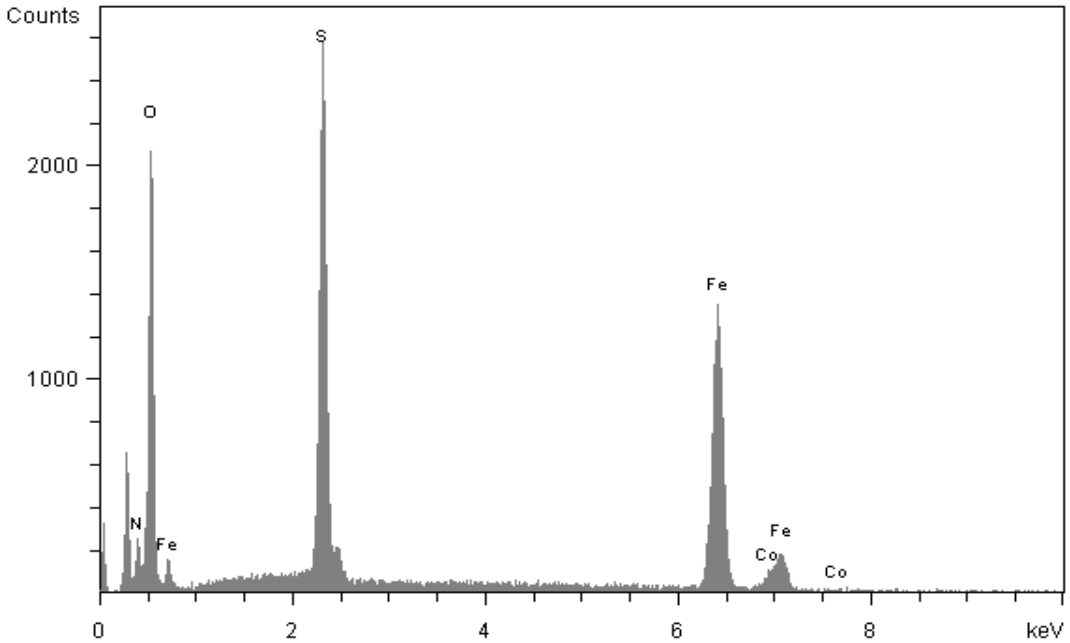

Figure A-3: EDX of each element of fragment 3 in iron oxide precipitate at pH 8, 35ºC, and 2 hours

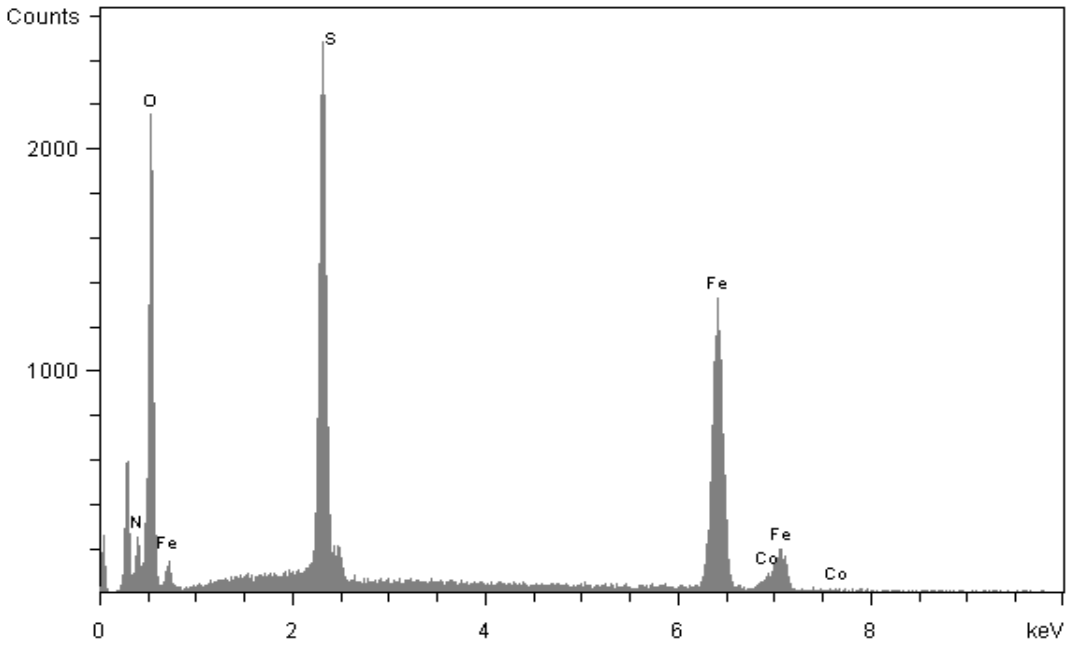

Figure A-4: EDX of each element of fragment 3 in iron oxide precipitate at pH 8, 35ºC, and 2 hours

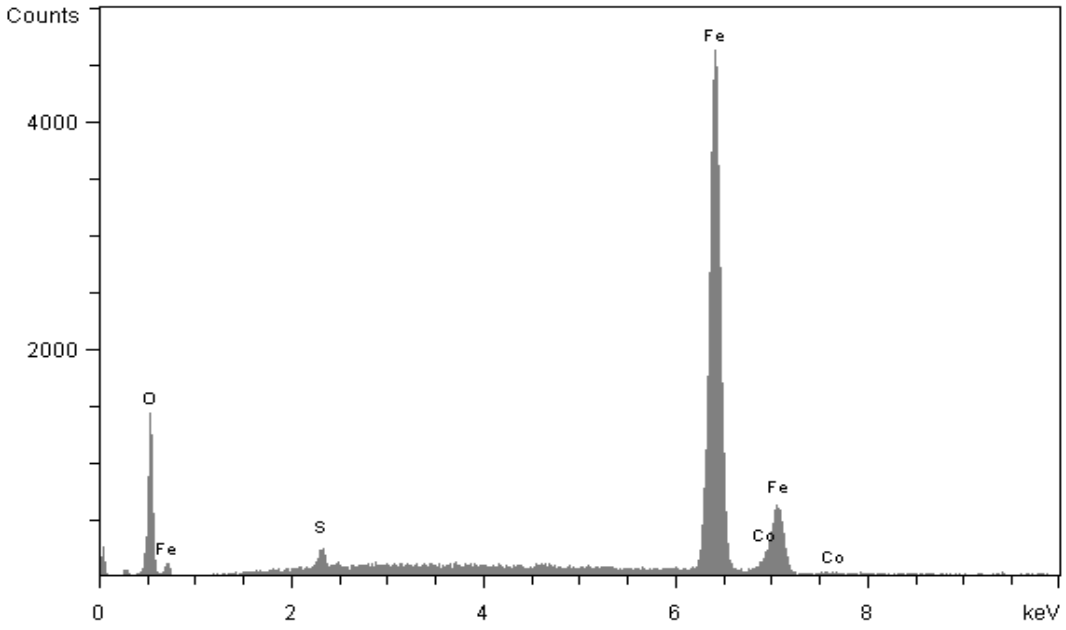

Figure A-5: EDX of each element of fragment 1 in iron oxide precipitate at pH 10, 35ºC, and 2 hours

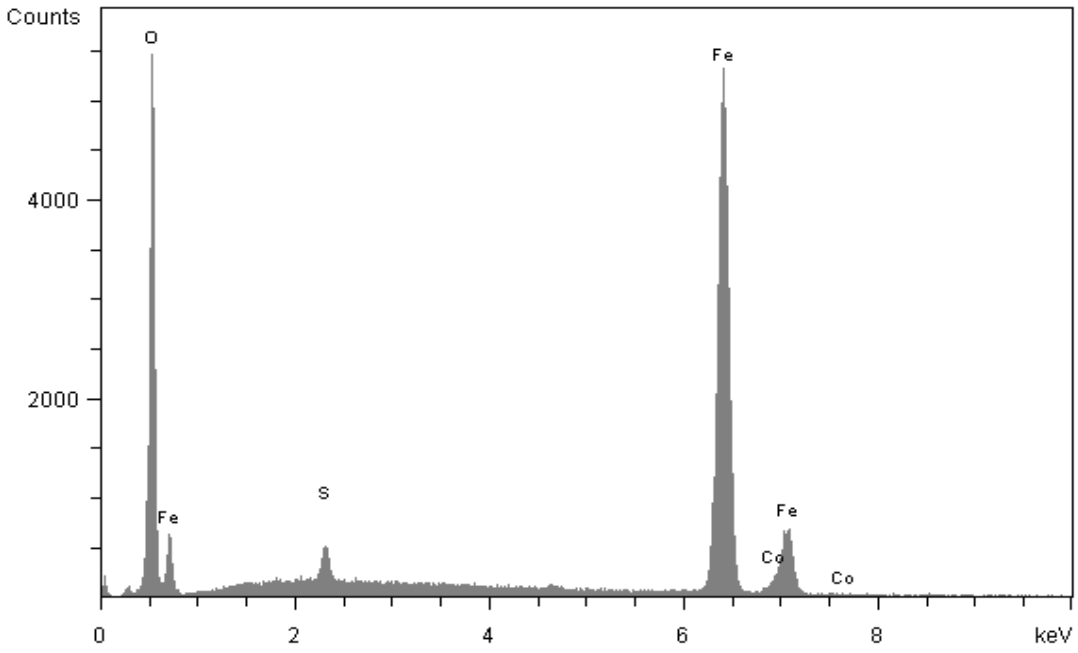

Figure A-6: EDX of each element of fragment 2 in iron oxide precipitate at pH 10, 35ºC, and 2 hours

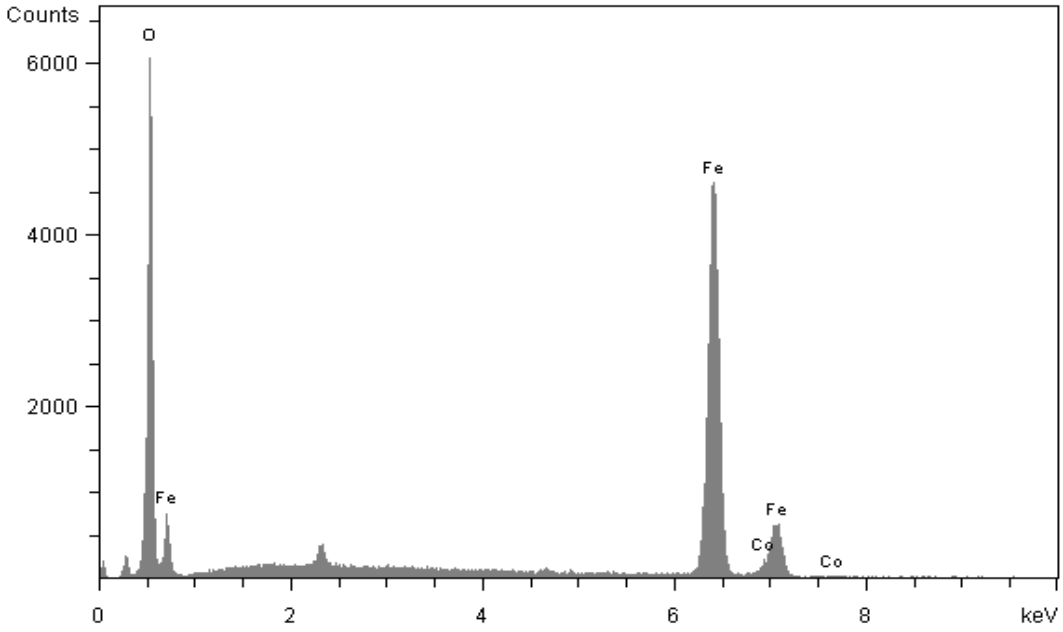

Figure A-7: EDX of each element of fragment 3 in iron oxide precipitate at pH 10, 35ºC, and 2 hours